Article:
Dalsøren, Stig B., Myhre, Gunnar, Hodnebrog, Øivind et al. (14 more authors) (2018) Discrepancy between simulated and observed ethane and propane levels explained by underestimated fossil emissions. Nature Geoscience. pp. 178-184. ISSN 1752-0908

https://doi.org/10.1038/s41561-018-0073-0

Discrepancy between simulated and observed ethane and propane levels explained by underestimated fossil emissions

Stig B. Dalsøren[1,*], Gunnar Myhre[2], Øivind Hodnebrog[2], Cathrine Lund Myhre[3], Andreas Stohl[3], Ignacio Pisso[3], Stefan Schwietzke[4,5], Lena Höglund-Isaksson[6], Detlev Helmig[7], Stefan Reimann[8], Stéphane Sauvage[9], Norbert Schmidbauer[3], Katie A. Read[10], Lucy J. Carpenter[10], Alastair C. Lewis[10], Shalini Punjabi[10] and Markus Wallasch[11]

[1]CICERO-Center for International Climate and Environmental Research Oslo, 0318, Oslo, Norway. Now at Institute for Marine Research, Flødevigen, 4817 His, Norway.

[2]CICERO-Center for International Climate and Environmental Research Oslo, 0318, Oslo, Norway.

[3]NILU-Norwegian Institute for Air Research, 2027 Kjeller, Norway.

[4]CIRES-Cooperative Institute for Research in Environmental Sciences, University of Colorado, Boulder, Colorado 80309, USA.

[5]NOAA Earth System Research Laboratory, Global Monitoring Division, Boulder, Colorado 80305-3337, USA.

[6]International Institute for Applied Systems Analysis, A-2361 Laxenburg, Austria.

[7]Institute of Arctic and Alpine Research, University of Colorado, Boulder, Colorado 80305, USA.

[8]Empa, Laboratory for Air Pollution/Environmental Technology, Swiss Federal Laboratories for Materials Science and Technology, 8600 Dübendorf, Switzerland.

[9]IMT Lille Douai, Univ. Lille, SAGE - Département Sciences de l'Atmosphère et Génie de l'Environnement, 59000 Lille, France.

[10]Wolfson Atmospheric Chemistry Laboratories, Department of Chemistry, University of York, Heslington, York, YO10 5DD, United Kingdom.

[11]Umweltbundesamt, Messnetzzentrale Langen, D-63225 Langen, Germany.

*e-mail: stig.dalsoeren@hi.no

Propane emissions

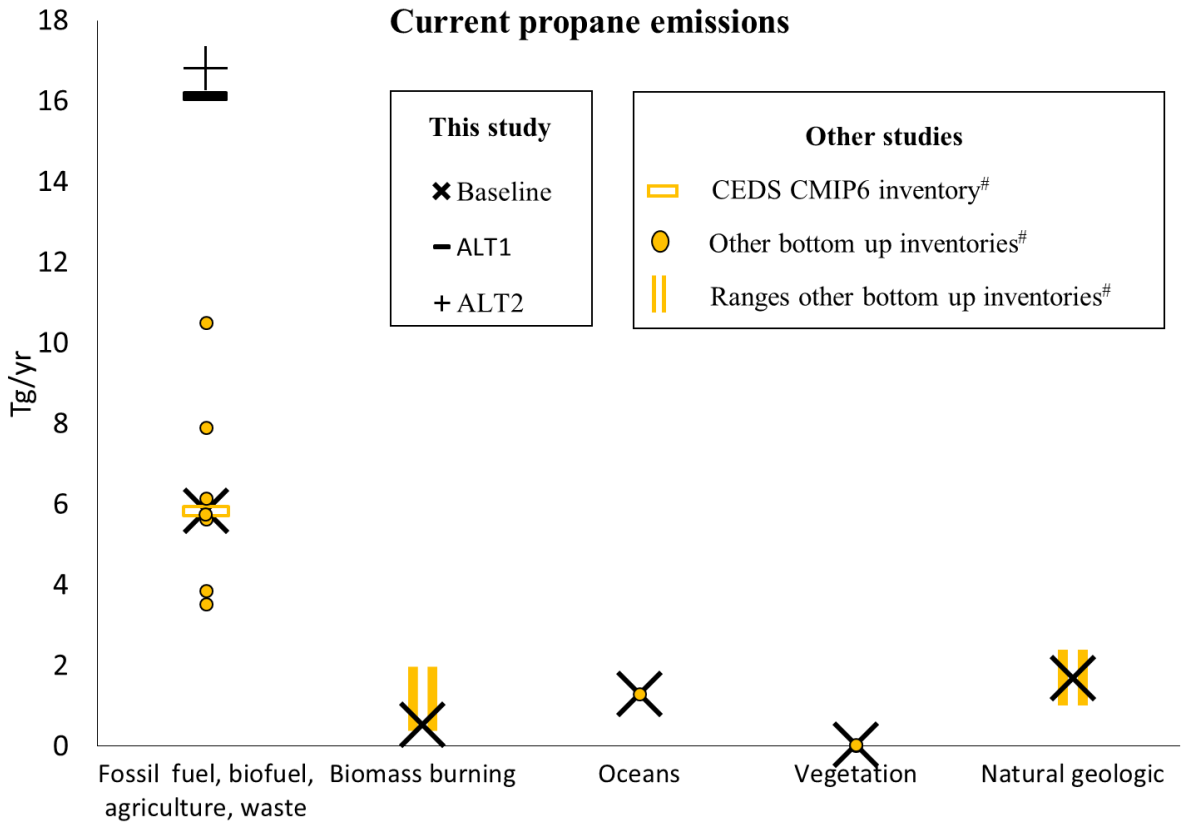

Figure S1: Global total sectoral propane emissions in the year 2011 baseline and alternative (ALT1, ALT2) simulations in this study (black symbols) compared to other studies (yellow). The inventories cover the year 2000 and onwards. The closest year to our simulation year 2011 is chosen for inventories not covering that year. Bottom up inventories (yellow symbols and bars)[#]: Fossil fuel, biofuel, agriculture, waste: CEDS CMIP6[1] (used in baseline in this study), HTAPv2, Edgar 3.2 FT, RETRO, POET, CMIP5 (average of MACCITY, ACCMIP, RCP2.6, RCP4.5, RCP6, RCP8.5) (as reported and referenced in ECCAD database: http://eccad.aeris-data.fr/), ARCTAS (as reported by ref. 2), EDGAR4.3.2 (as reported by ref. 3), and new inventory in ref. 4. Biomass burning: GFEDv4 (as used in baseline in this study), GICC, ACCMIP, POET, GFASv1.2, MACCITY, RETRO, RCP2.6, RCP4.5, RCP8.5 (as reported and referenced in ECCAD database: http://eccad.aeris-data.fr/), and FINN (as reported by ref. 5,6). Oceans: RETRO (used in baseline in this study). Vegetation: MEGAN-MACC (used in baseline this study), and MEGANv2 (as reported and referenced in ECCAD database: http://eccad.aeris-data.fr/). Geologic: As reported by ref. 7 (median estimate used in baseline in this study).

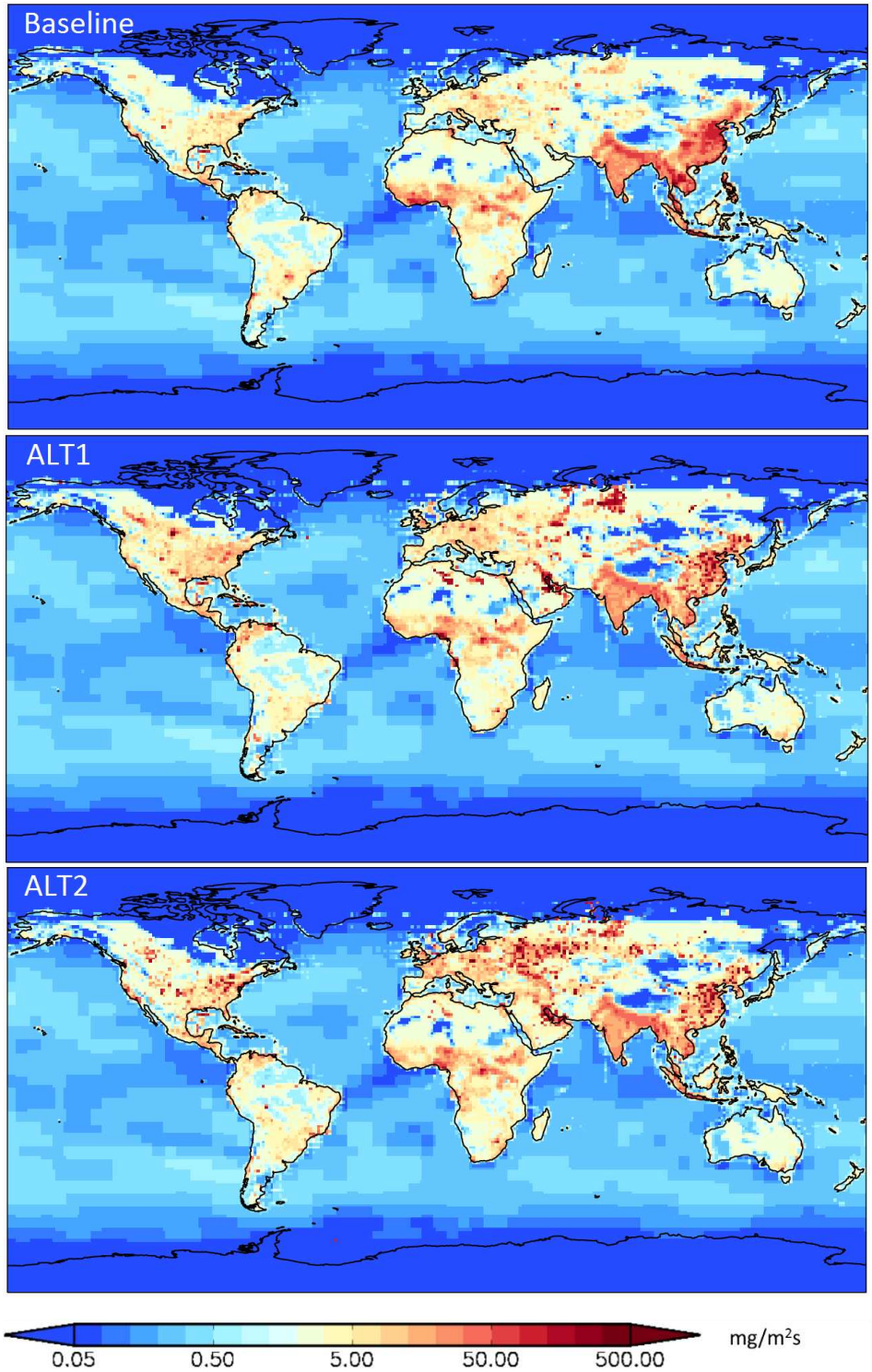

Figure S2: Ethane emissions (mg/m^{2}s) in the baseline (upper map), ALT1 (mid panel), and ALT2 (lower map) inventories in March 2011. (A logarithmic color scale is used.)

Sensitivity studies preindustrial conditions

Sensitivity simulations with meteorological input data for a different year and an alternative inventory for biomass burning emissions (see Methods) resulted in similar Antarctic concentrations and identical (meteorological sensitivity simulation) and 15 % lower (biomass burning sensitivity simulation) inter-polar ratio.

Comparison of atmospheric mole fraction measurements with Baseline 2011 and ALT2 simulations

a)

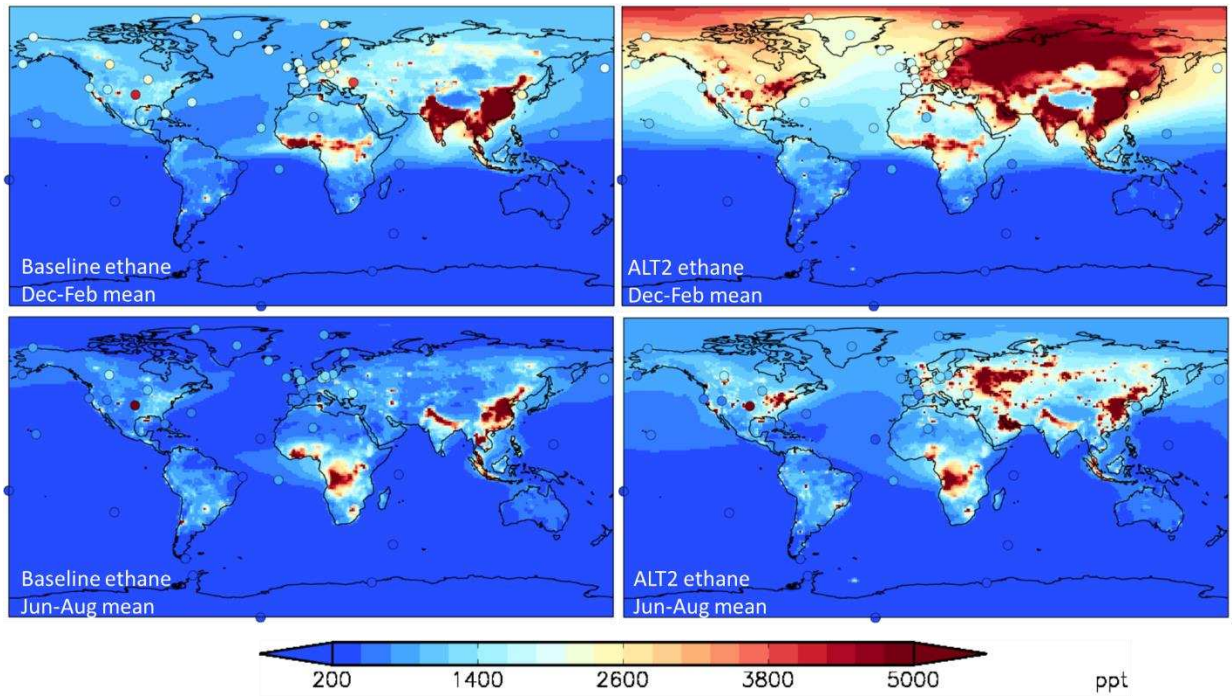

b)

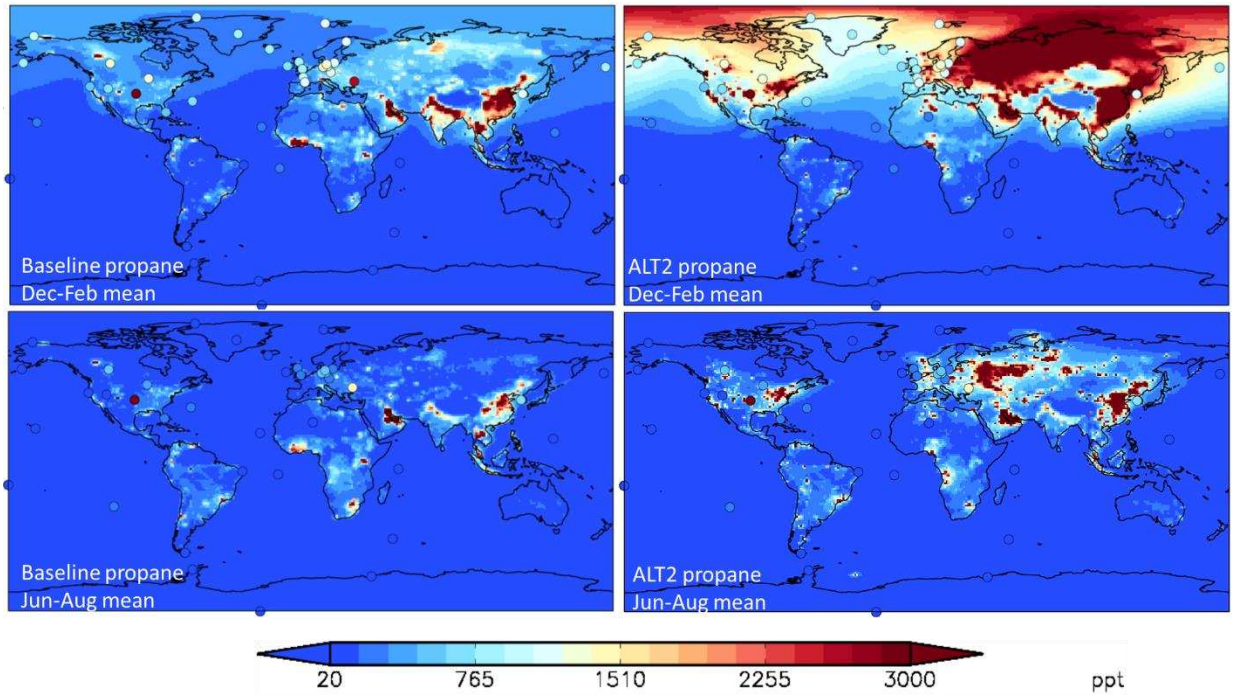

Figure S3: Comparison of modeled (background colours) and observed (colour-filled circles) surface ethane (ppt) for the year 2011. Model data for the lowest model layer was used. Stations with less than 6 samples within the 3 month averaging period were excluded from the comparison. Mountain stations that typically sample free tropospheric air and that are situated in areas where the model resolution doesn't resolve the terrain were also excluded. Details on the applied observation datasets are found in the Methods section. b) Same for propane.

Comparison year 2011 simulations with measurements for regions and individual stations

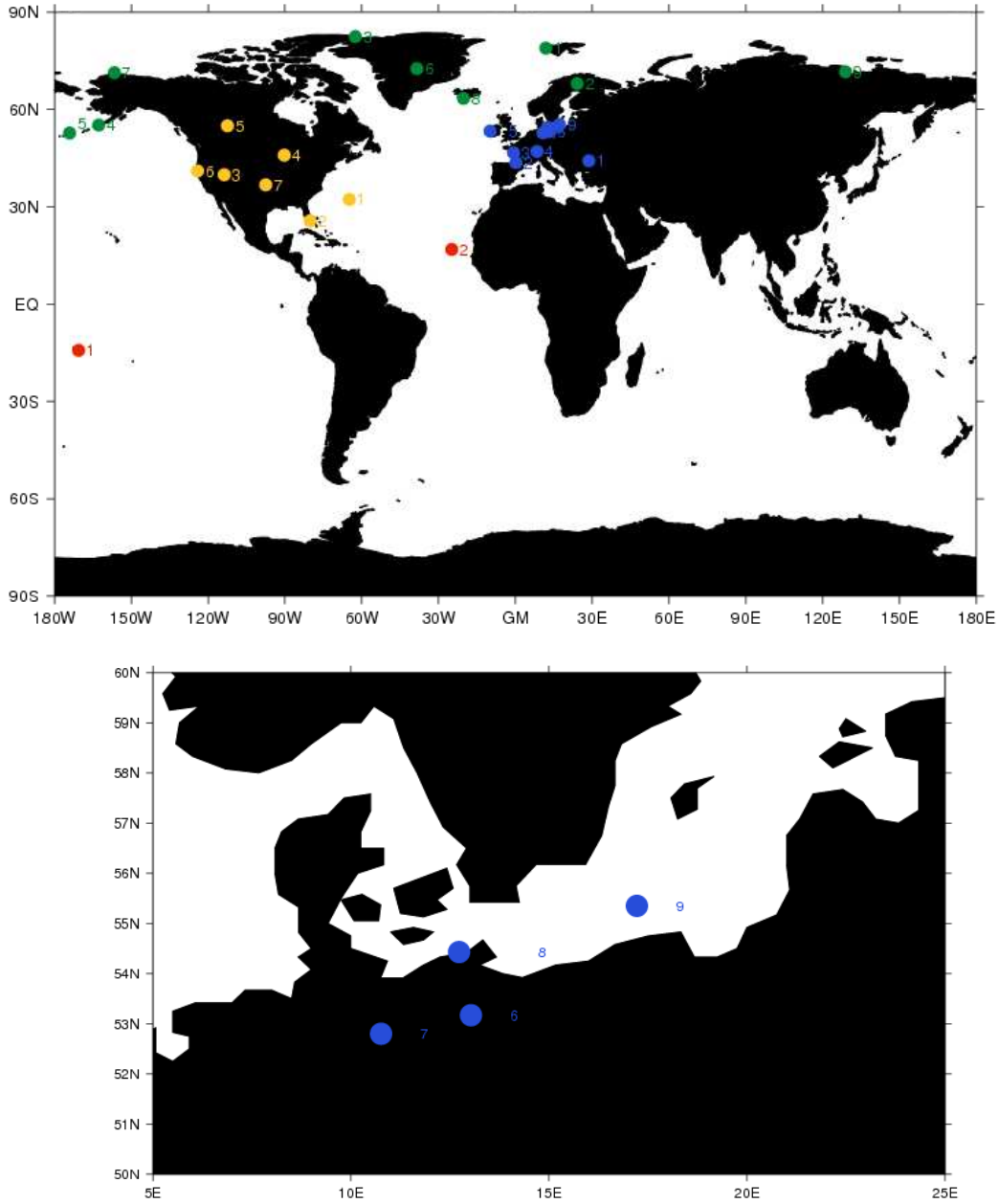

Figure S4: Upper map: Stations selected (criteria see Methods) for comparisons in Figures S5-9. The Arctic (green dots, Figure S5), U.S/Canada (yellow dots, Figure S6), and Europe (blue dots, Figure S7) have a sufficient number of stations to discuss regional patterns (main text and Tables S1-S2). Red dots are other interesting stations discussed in the main text and shown in Figures S8-S9 (Cape Verde, Samoa). Lower map: Zooming in on stations in northern central Europe.

Table S1: Information on measurement stations shown in Figure S4.

Region	Number	Station name	Latitude	Longitude	Altitude (m)
Arctic	1	Zeppelin Observatory	78.90N	11.88E	475
	2	Pallas	67.97N	24.12E	560
	3	Alert	82.45N	62.52W	210
	4	Cold Bay	55.20N	162.72W	25
	5	Shemya Island	52.72N	174.08E	40
	6	Summit	72.58N	38.48W	3238
	7	Barrow	71.32N	156.60W	11
	8	Heimaey	63.40N	20.28W	100
	9	Tiksi	71.59N	128.92E	43
U.S and Canada	1	Tudor Hill	32.27N	64.87W	30
	2	Key Biscayne	25.67N	80.20W	3
	3	Wendover	39.88N	113.72W	1320
	4	Park Falls	45.92N	90.27W	868
	5	Lac la Biche	54.95N	112.45W	540
	6	Trinidad Head	41.05N	124.15W	120
	7	Southern Great Plains	36.78N	97.50W	314
Europe	1	Black Sea	44.17N	28.67E	3
	2	Peyrusse Vieille	43.62N	0.18E	200
	3	La Tardière	46.65N	0.75W	133
	4	Rigi	47.07N	8.46E	1031
	5	Mace Head	53.33N	9.90W	8
	6	Waldhof	52.80N	10.76E	74
	7	Neuglobsow	53.17N	13.03E	62
	8	Zingst	54.43N	12.73E	1
	9	Baltic Sea	55.35N	17.22E	28
Other	1	Tutuila	14.24S	170.57W	42
	2	Cape Verde	16.85N	24.87W	10

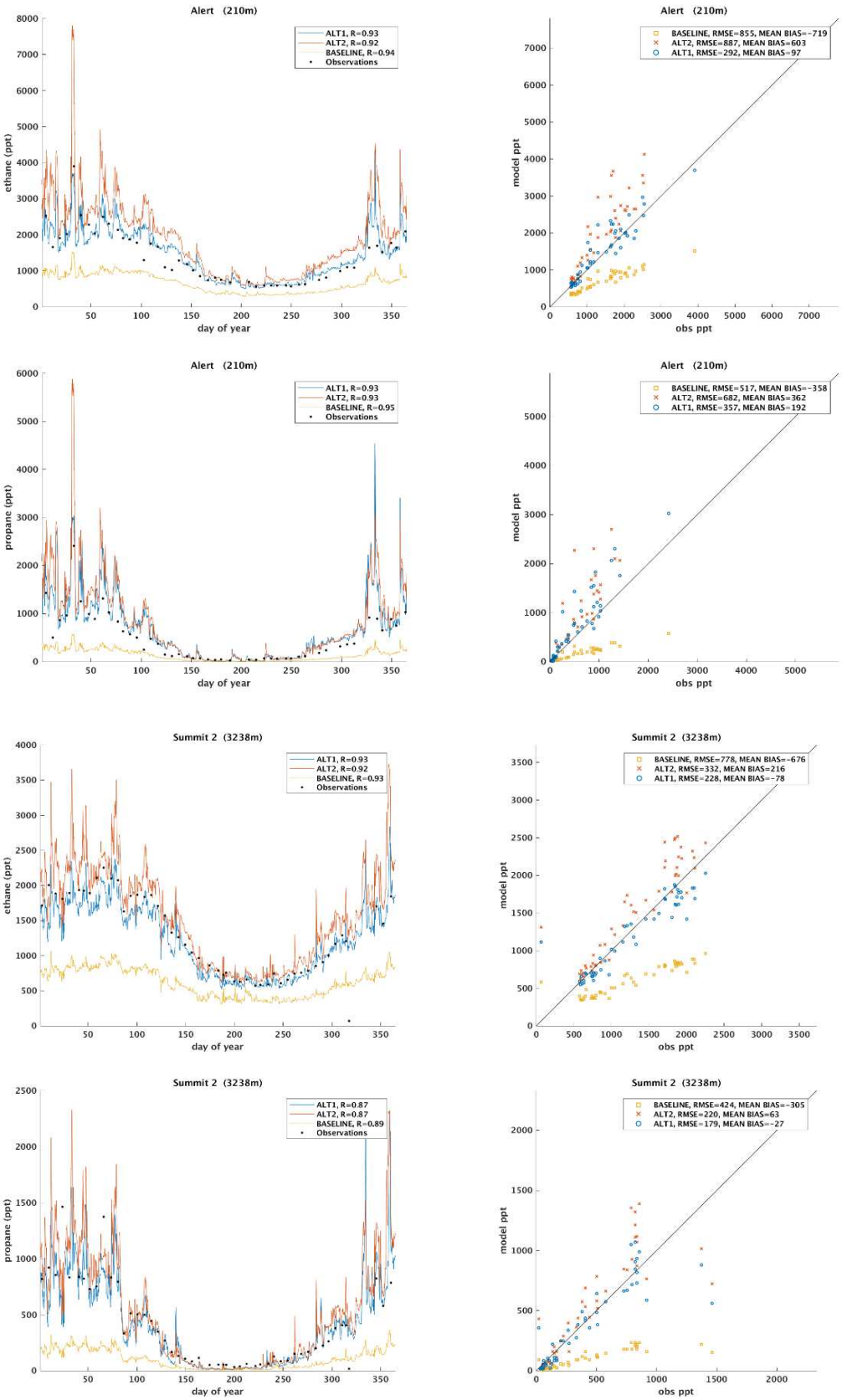
Alert (210m)
ALT1, R=0.93
ALT2, R=0.92
BASELINE, R=0.94
Observations
ethane (ppt)
day of year
Alert (210m)
BASELINE, RMSE=855, MEAN BIAS=-719
ALT2, RMSE=887, MEAN BIAS=603
ALT1, RMSE=292, MEAN BIAS=97
model ppt
obs ppt
Alert (210m)
ALT1, R=0.93
ALT2, R=0.93
BASELINE, R=0.95
Observations
propane (ppt)
day of year
Alert (210m)
BASELINE, RMSE=517, MEAN BIAS=-358
ALT2, RMSE=682, MEAN BIAS=362
ALT1, RMSE=357, MEAN BIAS=192
model ppt
obs ppt
Summit 2 (3238m)
ALT1, R=0.93
ALT2, R=0.92
BASELINE, R=0.93
Observations
ethane (ppt)
day of year
Summit 2 (3238m)
BASELINE, RMSE=778, MEAN BIAS=-676
ALT2, RMSE=332, MEAN BIAS=216
ALT1, RMSE=228, MEAN BIAS=-78
model ppt
obs ppt
Summit 2 (3238m)
ALT1, R=0.87
ALT2, R=0.87
BASELINE, R=0.89
Observations
propane (ppt)
day of year
Summit 2 (3238m)
BASELINE, RMSE=424, MEAN BIAS=-305
ALT2, RMSE=220, MEAN BIAS=63
ALT1, RMSE=179, MEAN BIAS=-27
model ppt
obs ppt

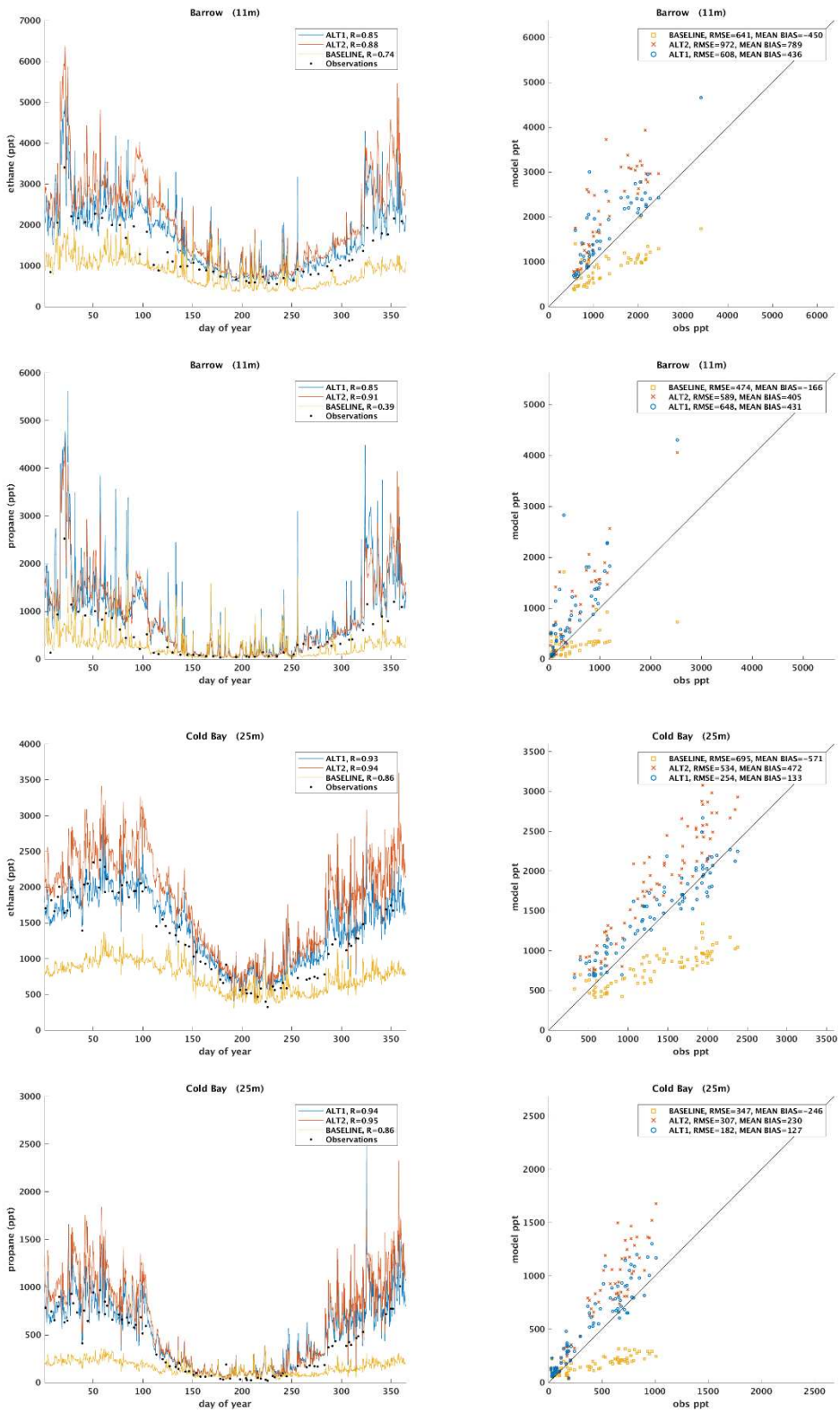
Barrow (11m)
ALT1, R=0.85
ALT2, R=0.88
BASELINE, R=0.74
Observations
ethane (ppt)
day of year
Barrow (11m)
BASELINE, RMSE=641, MEAN BIAS=-450
ALT2, RMSE=972, MEAN BIAS=789
ALT1, RMSE=608, MEAN BIAS=436
model ppt
obs ppt
Barrow (11m)
ALT1, R=0.85
ALT2, R=0.91
BASELINE, R=0.39
Observations
propane (ppt)
day of year
Barrow (11m)
BASELINE, RMSE=474, MEAN BIAS=-166
ALT2, RMSE=589, MEAN BIAS=405
ALT1, RMSE=648, MEAN BIAS=431
model ppt
obs ppt
Cold Bay (25m)
ALT1, R=0.93
ALT2, R=0.94
BASELINE, R=0.86
Observations
ethane (ppt)
day of year
Cold Bay (25m)
BASELINE, RMSE=695, MEAN BIAS=-571
ALT2, RMSE=534, MEAN BIAS=472
ALT1, RMSE=254, MEAN BIAS=133
model ppt
obs ppt
Cold Bay (25m)
ALT1, R=0.94
ALT2, R=0.95
BASELINE, R=0.86
Observations
propane (ppt)
day of year
Cold Bay (25m)
BASELINE, RMSE=347, MEAN BIAS=-246
ALT2, RMSE=307, MEAN BIAS=230
ALT1, RMSE=182, MEAN BIAS=127
model ppt
obs ppt

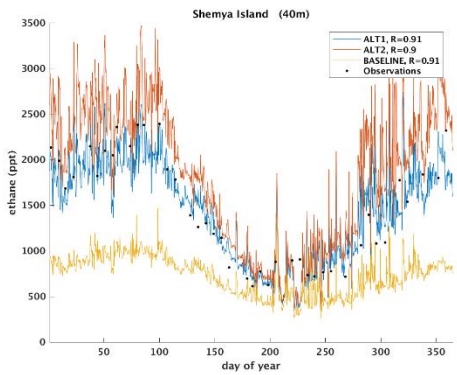
Shemya Island (40m)
ALT1, R=0.91
ALT2, R=0.9
BASELINE, R=0.91
Observations
ethane (ppt)
day of year

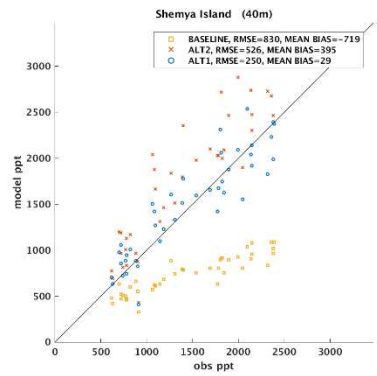
Shemya Island (40m)
BASELINE, RMSE=830, MEAN BIAS=-719
ALT2, RMSE=526, MEAN BIAS=395
ALT1, RMSE=250, MEAN BIAS=29
model ppt
obs ppt

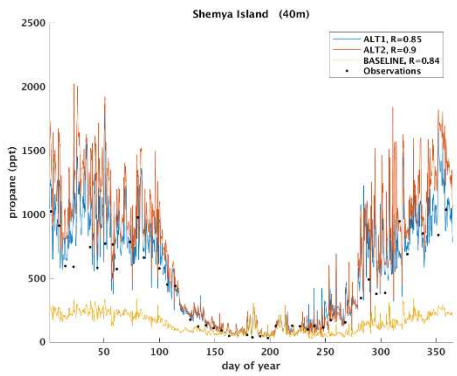
Shemya Island (40m)
ALT1, R=0.85
ALT2, R=0.9
BASELINE, R=0.84
Observations
propane (ppt)
day of year

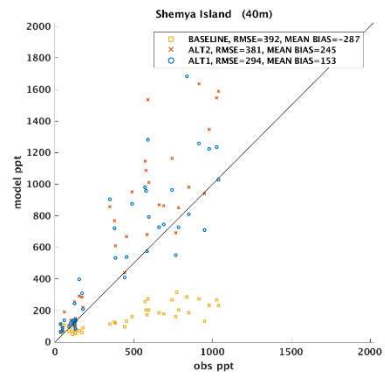
Shemya Island (40m)
BASELINE, RMSE=392, MEAN BIAS=-287
ALT2, RMSE=381, MEAN BIAS=245
ALT1, RMSE=294, MEAN BIAS=153
model ppt
obs ppt

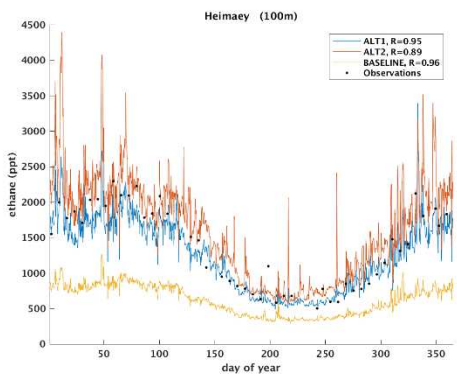
Heimaey (100m)
ALT1, R=0.95
ALT2, R=0.89
BASELINE, R=0.96
Observations
ethane (ppt)
day of year

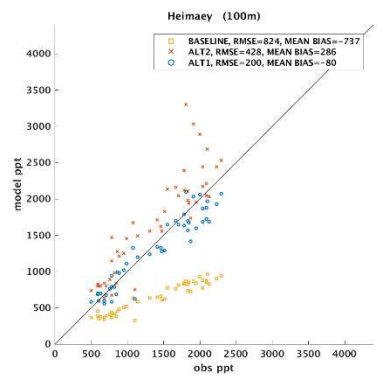
Heimaey (100m)
BASELINE, RMSE=824, MEAN BIAS=-737
ALT2, RMSE=428, MEAN BIAS=286
ALT1, RMSE=200, MEAN BIAS=-80
model ppt
obs ppt

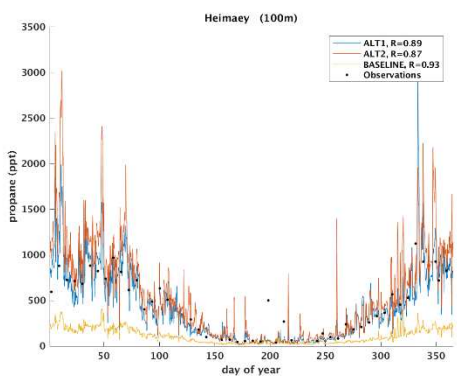
Heimaey (100m)
ALT1, R=0.89
ALT2, R=0.87
BASELINE, R=0.93
Observations
propane (ppt)
day of year

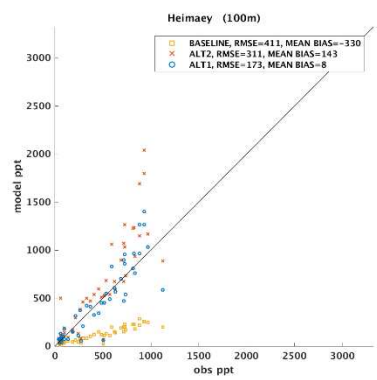
Heimaey (100m)
BASELINE, RMSE=411, MEAN BIAS=-330
ALT2, RMSE=311, MEAN BIAS=143
ALT1, RMSE=173, MEAN BIAS=8
model ppt
obs ppt

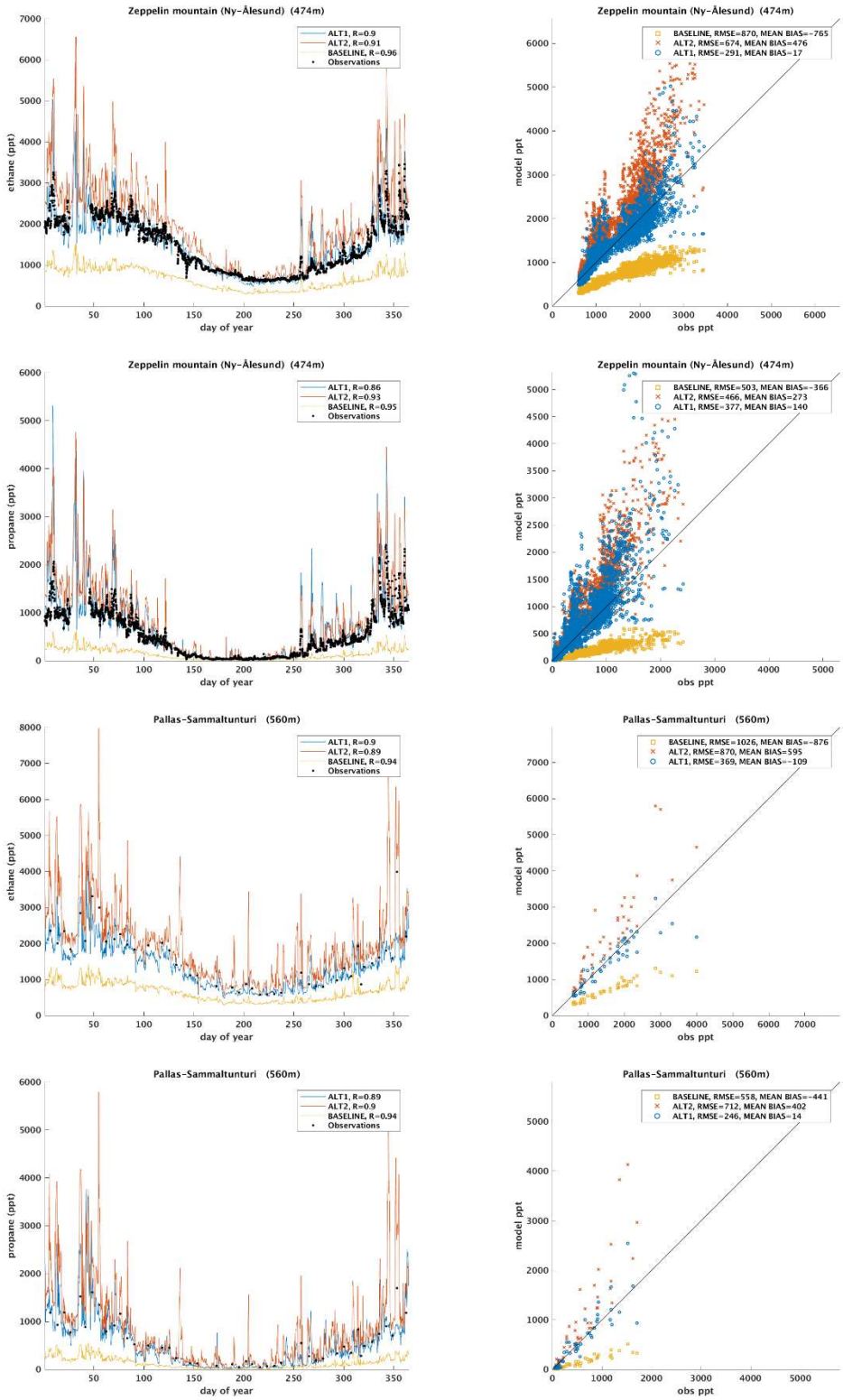
Zeppelin mountain (Ny-Ålesund) (474m)
ALT1, R=0.9
ALT2, R=0.91
BASELINE, R=0.96
Observations
ethane (ppt)
day of year
Zeppelin mountain (Ny-Ålesund) (474m)
BASELINE, RMSE=870, MEAN BIAS=-765
ALT2, RMSE=674, MEAN BIAS=476
ALT1, RMSE=291, MEAN BIAS=17
model ppt
obs ppt
Zeppelin mountain (Ny-Ålesund) (474m)
ALT1, R=0.86
ALT2, R=0.93
BASELINE, R=0.95
Observations
propane (ppt)
day of year
Zeppelin mountain (Ny-Ålesund) (474m)
BASELINE, RMSE=503, MEAN BIAS=-366
ALT2, RMSE=466, MEAN BIAS=273
ALT1, RMSE=377, MEAN BIAS=140
model ppt
obs ppt
Pallas-Sammaltunturi (560m)
ALT1, R=0.9
ALT2, R=0.89
BASELINE, R=0.94
Observations
ethane (ppt)
day of year
Pallas-Sammaltunturi (560m)
BASELINE, RMSE=1026, MEAN BIAS=-876
ALT2, RMSE=870, MEAN BIAS=595
ALT1, RMSE=369, MEAN BIAS=-109
model ppt
obs ppt
Pallas-Sammaltunturi (560m)
ALT1, R=0.89
ALT2, R=0.9
BASELINE, R=0.94
Observations
propane (ppt)
day of year
Pallas-Sammaltunturi (560m)
BASELINE, RMSE=558, MEAN BIAS=-441
ALT2, RMSE=712, MEAN BIAS=402
ALT1, RMSE=246, MEAN BIAS=14
model ppt
obs ppt

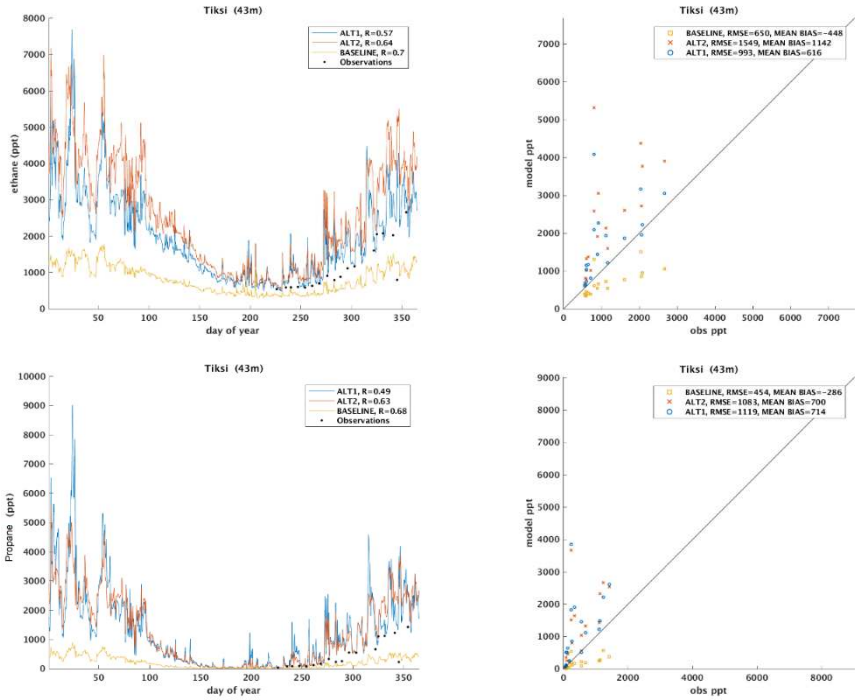

Figure S5: Comparison of modeled and observed ethane and propane for Arctic stations for the year 2011. Zeppelin data were collected under the framework ACTRIS, and the remaining sites are reported to GAW-WDCGG under NOAA/INSTAAR, and were accessed in May 2017.

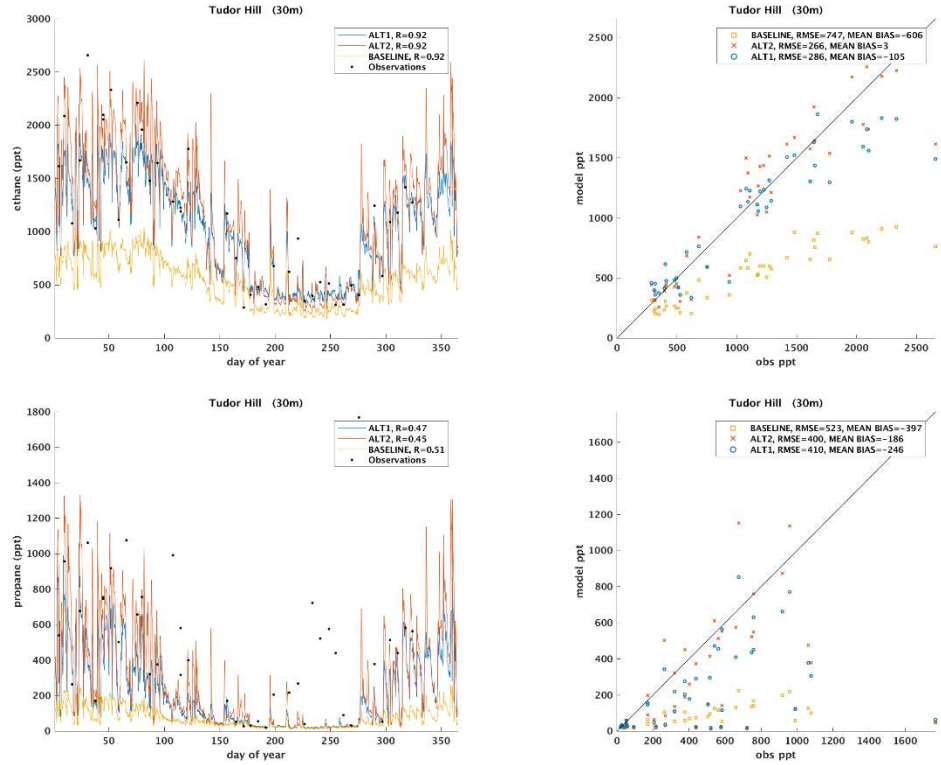

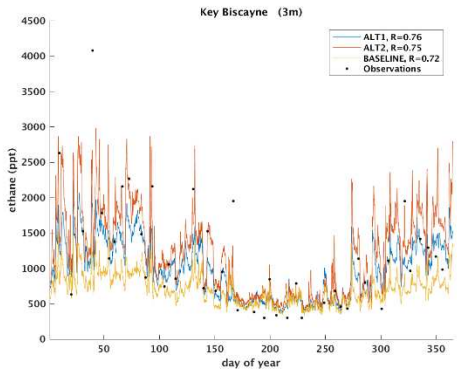
Key Biscayne (3m)
ALT1, R=0.76
ALT2, R=0.75
BASELINE, R=0.72
Observations
ethane (ppt)
day of year

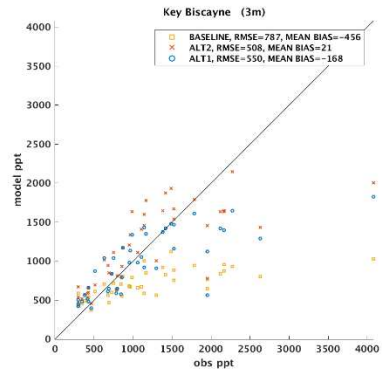
Key Biscayne (3m)
BASELINE, RMSE=787, MEAN BIAS=-456
ALT2, RMSE=508, MEAN BIAS=21
ALT1, RMSE=550, MEAN BIAS=-168
model ppt
obs ppt

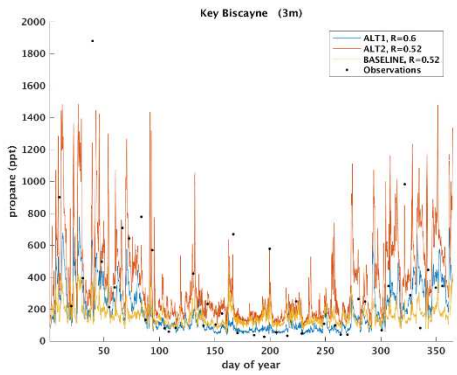
Key Biscayne (3m)
ALT1, R=0.6
ALT2, R=0.52
BASELINE, R=0.52
Observations
propane (ppt)
day of year

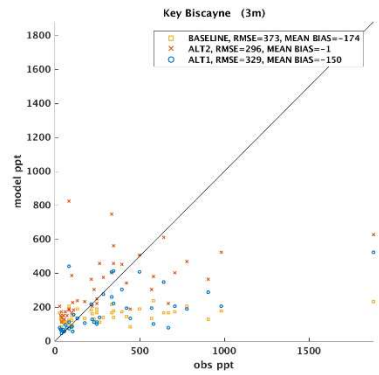
Key Biscayne (3m)
BASELINE, RMSE=373, MEAN BIAS=-174
ALT2, RMSE=296, MEAN BIAS=-1
ALT1, RMSE=329, MEAN BIAS=-150
model ppt
obs ppt

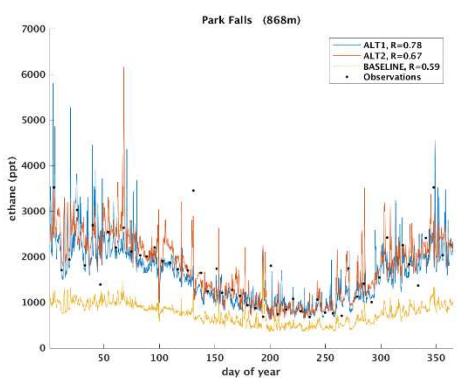
Park Falls (868m)
ALT1, R=0.78
ALT2, R=0.67
BASELINE, R=0.59
Observations
ethane (ppt)
day of year

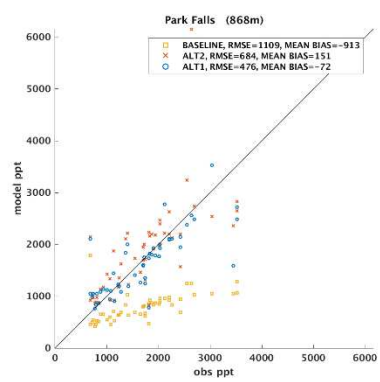
Park Falls (868m)
BASELINE, RMSE=1109, MEAN BIAS=-913
ALT2, RMSE=684, MEAN BIAS=151
ALT1, RMSE=476, MEAN BIAS=-72
model ppt
obs ppt

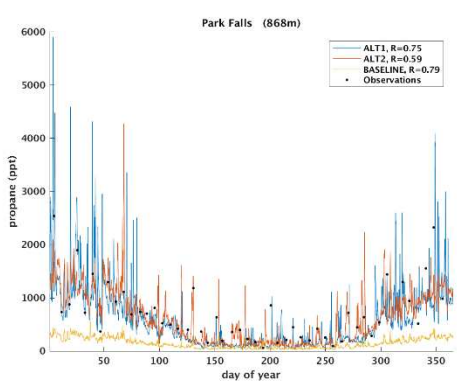
Park Falls (868m)
ALT1, R=0.75
ALT2, R=0.59
BASELINE, R=0.79
Observations
propane (ppt)
day of year

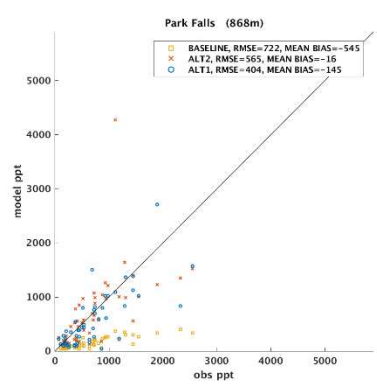
Park Falls (868m)
BASELINE, RMSE=722, MEAN BIAS=-545
ALT2, RMSE=565, MEAN BIAS=-16
ALT1, RMSE=404, MEAN BIAS=-145
model ppt
obs ppt

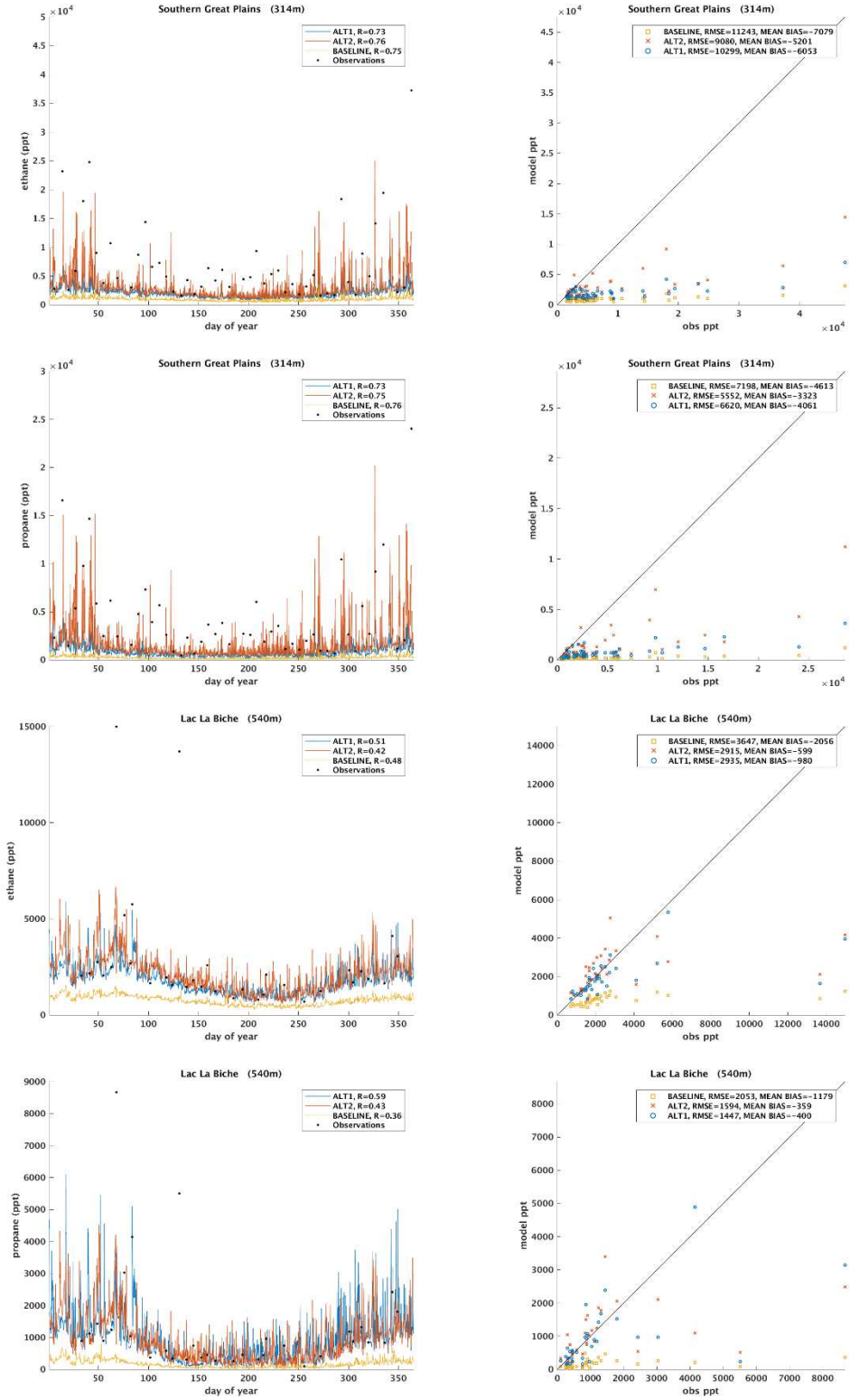
Southern Great Plains (314m)
ALT1, R=0.73
ALT2, R=0.76
BASELINE, R=0.75
Observations
ethane (ppt)
day of year
Southern Great Plains (314m)
BASELINE, RMSE=11243, MEAN BIAS=-7079
ALT2, RMSE=9080, MEAN BIAS=-5201
ALT1, RMSE=10299, MEAN BIAS=-6053
model ppt
obs ppt
Southern Great Plains (314m)
ALT1, R=0.73
ALT2, R=0.75
BASELINE, R=0.76
Observations
propane (ppt)
day of year
Southern Great Plains (314m)
BASELINE, RMSE=7198, MEAN BIAS=-4613
ALT2, RMSE=5552, MEAN BIAS=-3323
ALT1, RMSE=6620, MEAN BIAS=-4061
model ppt
obs ppt
Lac La Biche (540m)
ALT1, R=0.51
ALT2, R=0.42
BASELINE, R=0.48
Observations
ethane (ppt)
day of year
Lac La Biche (540m)
BASELINE, RMSE=3647, MEAN BIAS=-2056
ALT2, RMSE=2915, MEAN BIAS=-599
ALT1, RMSE=2935, MEAN BIAS=-980
model ppt
obs ppt
Lac La Biche (540m)
ALT1, R=0.59
ALT2, R=0.43
BASELINE, R=0.36
Observations
propane (ppt)
day of year
Lac La Biche (540m)
BASELINE, RMSE=2053, MEAN BIAS=-1179
ALT2, RMSE=1594, MEAN BIAS=-359
ALT1, RMSE=1447, MEAN BIAS=-400
model ppt
obs ppt

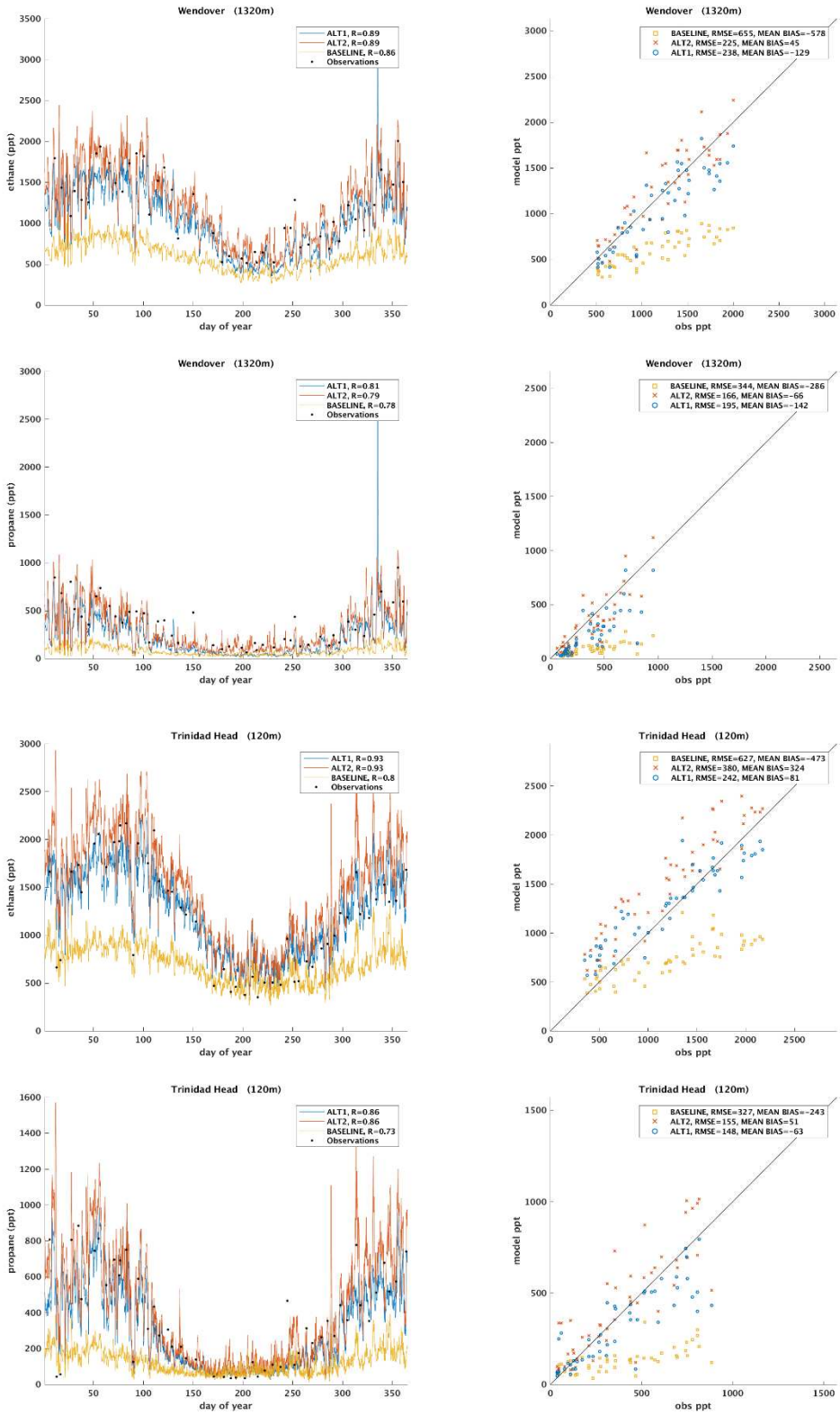

Figure S6: Comparison of modeled and observed ethane and propane for non-Arctic U.S and Canadian station for the year 2011. All stations are reported to GAW-WDCG under NOAA/INSTAAR, and were accessed May 2017.

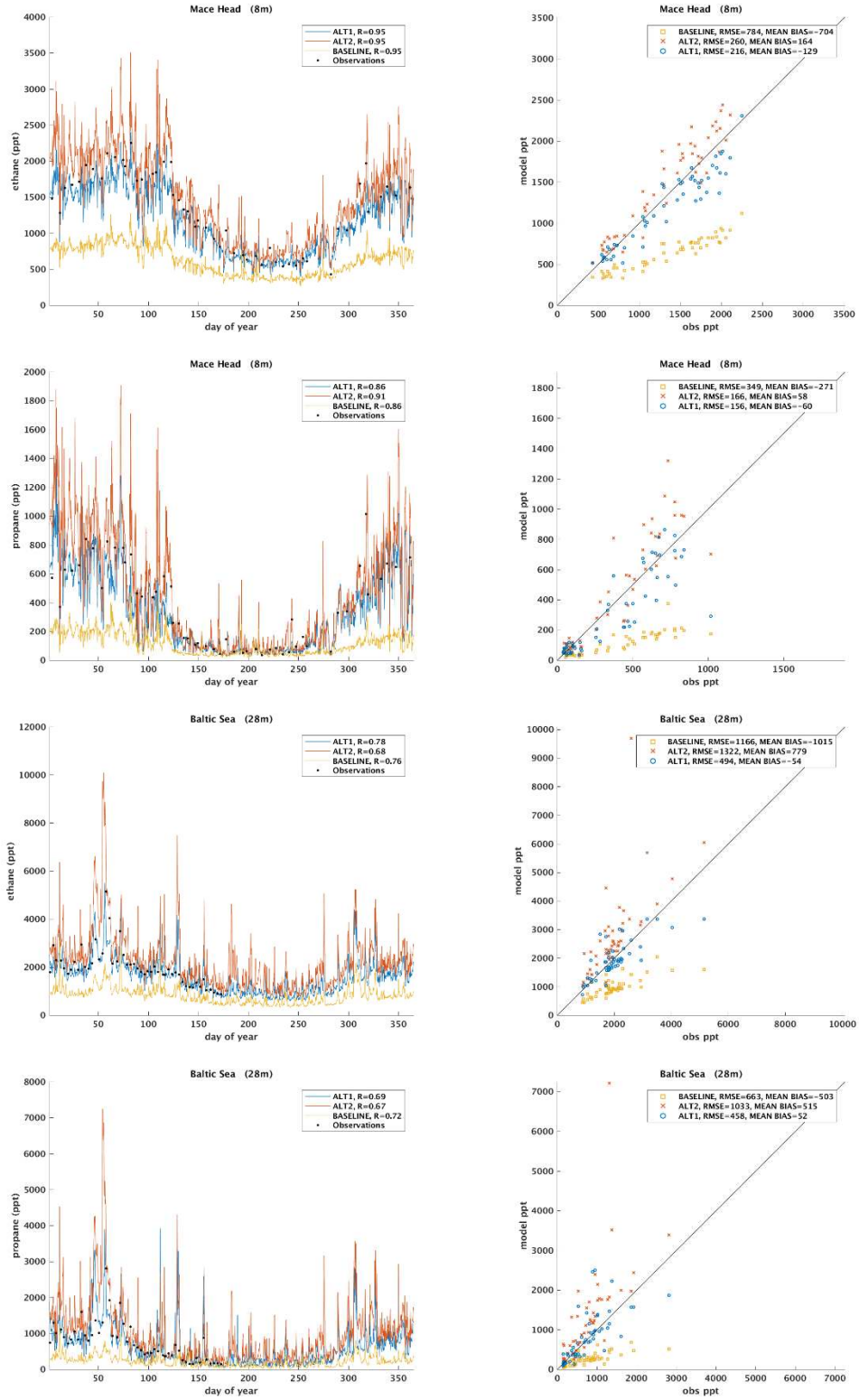
Mace Head (8m)
ALT1, R=0.95
ALT2, R=0.95
BASELINE, R=0.95
Observations
ethane (ppt)
day of year
Mace Head (8m)
BASELINE, RMSE=784, MEAN BIAS=-704
ALT2, RMSE=260, MEAN BIAS=164
ALT1, RMSE=216, MEAN BIAS=-129
model ppt
obs ppt
Mace Head (8m)
ALT1, R=0.86
ALT2, R=0.91
BASELINE, R=0.86
Observations
propane (ppt)
day of year
Mace Head (8m)
BASELINE, RMSE=349, MEAN BIAS=-271
ALT2, RMSE=166, MEAN BIAS=58
ALT1, RMSE=156, MEAN BIAS=-60
model ppt
obs ppt
Baltic Sea (28m)
ALT1, R=0.78
ALT2, R=0.68
BASELINE, R=0.76
Observations
ethane (ppt)
day of year
Baltic Sea (28m)
BASELINE, RMSE=1166, MEAN BIAS=-1015
ALT2, RMSE=1322, MEAN BIAS=779
ALT1, RMSE=494, MEAN BIAS=-54
model ppt
obs ppt
Baltic Sea (28m)
ALT1, R=0.69
ALT2, R=0.67
BASELINE, R=0.72
Observations
propane (ppt)
day of year
Baltic Sea (28m)
BASELINE, RMSE=663, MEAN BIAS=-503
ALT2, RMSE=1033, MEAN BIAS=515
ALT1, RMSE=458, MEAN BIAS=52
model ppt
obs ppt

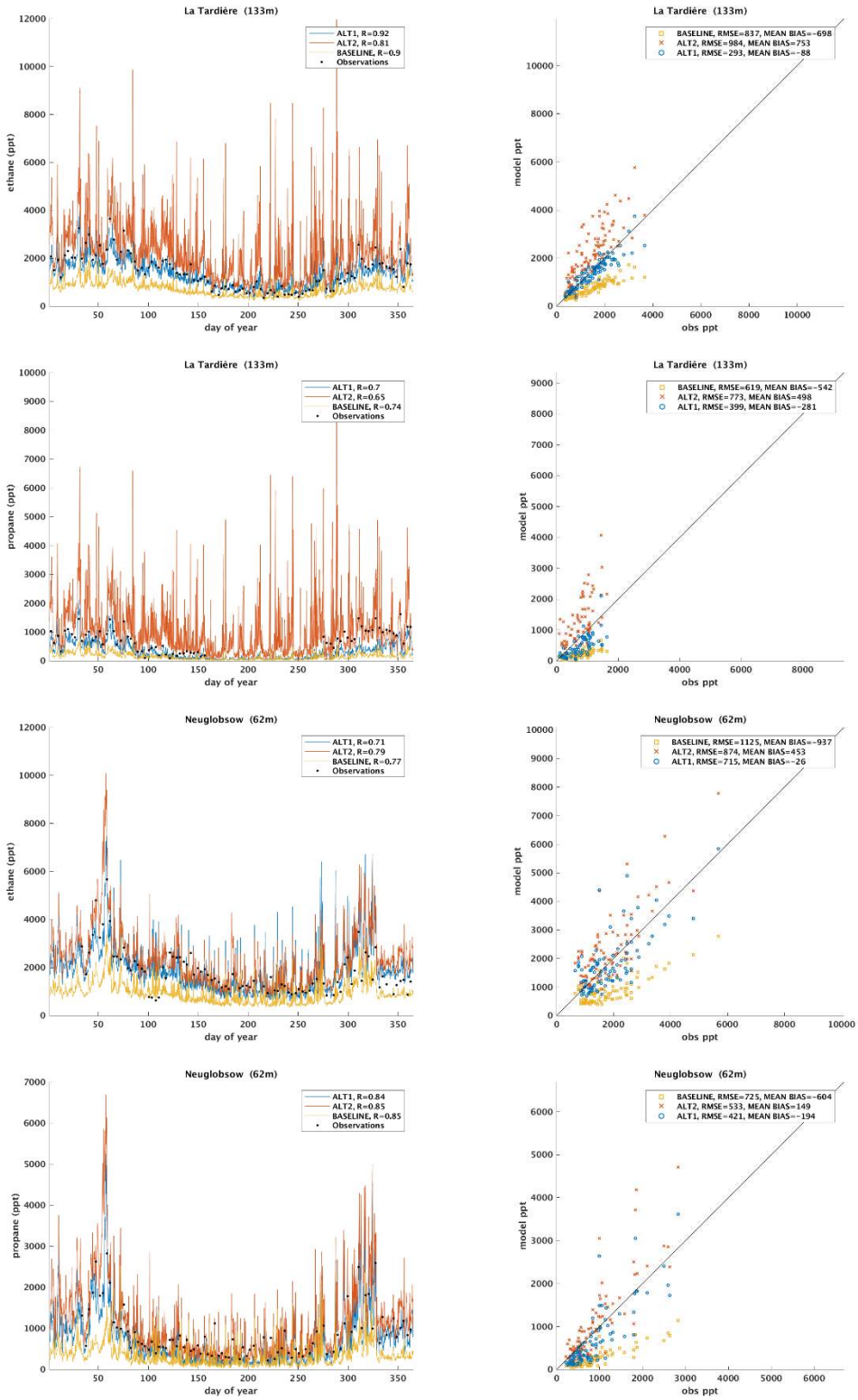
La Tardière (133m)
ALT1, R=0.92
ALT2, R=0.81
BASELINE, R=0.9
Observations
ethane (ppt)
day of year
La Tardière (133m)
BASELINE, RMSE=837, MEAN BIAS=-698
ALT2, RMSE=984, MEAN BIAS=753
ALT1, RMSE=293, MEAN BIAS=-88
model ppt
obs ppt
La Tardière (133m)
ALT1, R=0.7
ALT2, R=0.65
BASELINE, R=0.74
Observations
propane (ppt)
day of year
La Tardière (133m)
BASELINE, RMSE=619, MEAN BIAS=-542
ALT2, RMSE=773, MEAN BIAS=498
ALT1, RMSE=399, MEAN BIAS=-281
model ppt
obs ppt
Neuglobsow (62m)
ALT1, R=0.71
ALT2, R=0.79
BASELINE, R=0.77
Observations
ethane (ppt)
day of year
Neuglobsow (62m)
BASELINE, RMSE=1125, MEAN BIAS=-937
ALT2, RMSE=874, MEAN BIAS=453
ALT1, RMSE=715, MEAN BIAS=-26
model ppt
obs ppt
Neuglobsow (62m)
ALT1, R=0.84
ALT2, R=0.85
BASELINE, R=0.85
Observations
propane (ppt)
day of year
Neuglobsow (62m)
BASELINE, RMSE=725, MEAN BIAS=-604
ALT2, RMSE=533, MEAN BIAS=149
ALT1, RMSE=421, MEAN BIAS=-194
model ppt
obs ppt

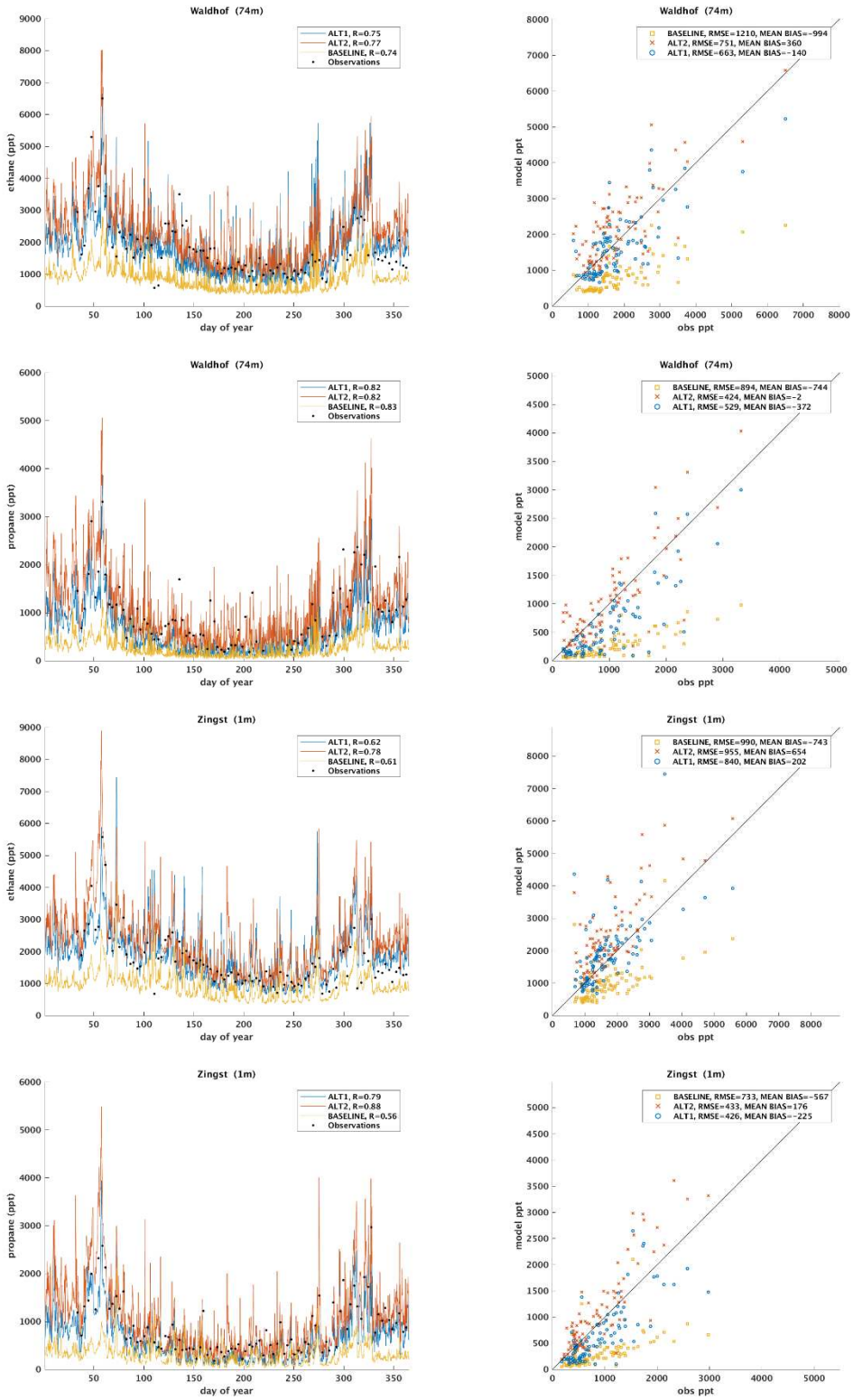
Waldhof (74m)
ALT1, R=0.75
ALT2, R=0.77
BASELINE, R=0.74
Observations
ethane (ppt)
day of year
Waldhof (74m)
BASELINE, RMSE=1210, MEAN BIAS=-994
ALT2, RMSE=751, MEAN BIAS=360
ALT1, RMSE=663, MEAN BIAS=-140
model ppt
obs ppt
Waldhof (74m)
ALT1, R=0.82
ALT2, R=0.82
BASELINE, R=0.83
Observations
propane (ppt)
day of year
Waldhof (74m)
BASELINE, RMSE=894, MEAN BIAS=-744
ALT2, RMSE=424, MEAN BIAS=-2
ALT1, RMSE=529, MEAN BIAS=-372
model ppt
obs ppt
Zingst (1m)
ALT1, R=0.62
ALT2, R=0.78
BASELINE, R=0.61
Observations
ethane (ppt)
day of year
Zingst (1m)
BASELINE, RMSE=990, MEAN BIAS=-743
ALT2, RMSE=955, MEAN BIAS=654
ALT1, RMSE=840, MEAN BIAS=202
model ppt
obs ppt
Zingst (1m)
ALT1, R=0.79
ALT2, R=0.88
BASELINE, R=0.56
Observations
propane (ppt)
day of year
Zingst (1m)
BASELINE, RMSE=733, MEAN BIAS=-567
ALT2, RMSE=433, MEAN BIAS=176
ALT1, RMSE=426, MEAN BIAS=-225
model ppt
obs ppt

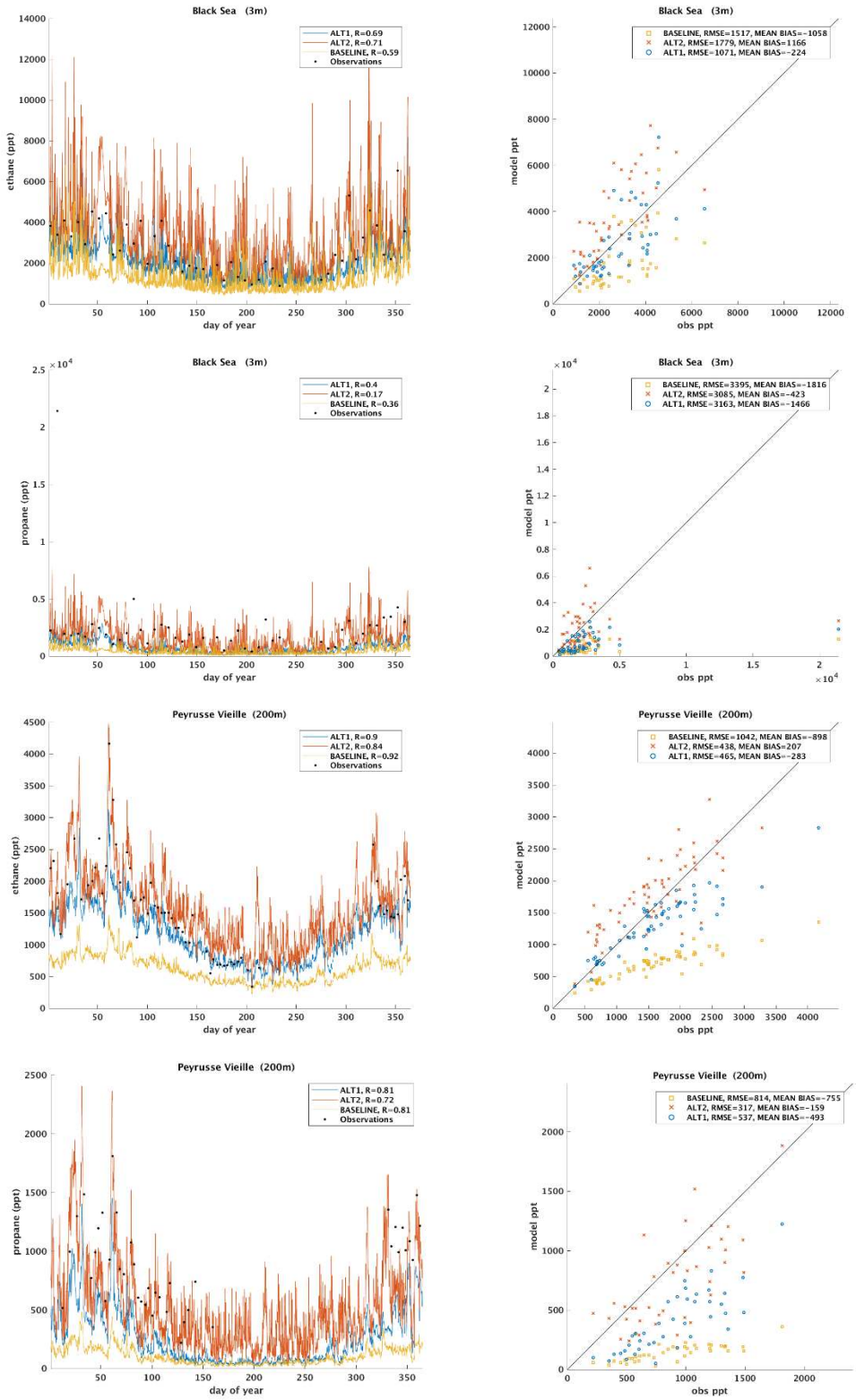
Black Sea (3m)
ALT1, R=0.69
ALT2, R=0.71
BASELINE, R=0.59
Observations
ethane (ppt)
day of year
Black Sea (3m)
BASELINE, RMSE=1517, MEAN BIAS=-1058
ALT2, RMSE=1779, MEAN BIAS=1166
ALT1, RMSE=1071, MEAN BIAS=-224
model ppt
obs ppt
Black Sea (3m)
ALT1, R=0.4
ALT2, R=0.17
BASELINE, R=0.36
Observations
propane (ppt)
day of year
Black Sea (3m)
BASELINE, RMSE=3395, MEAN BIAS=-1816
ALT2, RMSE=3085, MEAN BIAS=-423
ALT1, RMSE=3163, MEAN BIAS=-1466
model ppt
obs ppt
Peyrusse Vieille (200m)
ALT1, R=0.9
ALT2, R=0.84
BASELINE, R=0.92
Observations
ethane (ppt)
day of year
Peyrusse Vieille (200m)
BASELINE, RMSE=1042, MEAN BIAS=-898
ALT2, RMSE=438, MEAN BIAS=207
ALT1, RMSE=465, MEAN BIAS=-283
model ppt
obs ppt
Peyrusse Vieille (200m)
ALT1, R=0.81
ALT2, R=0.72
BASELINE, R=0.81
Observations
propane (ppt)
day of year
Peyrusse Vieille (200m)
BASELINE, RMSE=814, MEAN BIAS=-755
ALT2, RMSE=317, MEAN BIAS=-159
ALT1, RMSE=537, MEAN BIAS=-493
model ppt
obs ppt

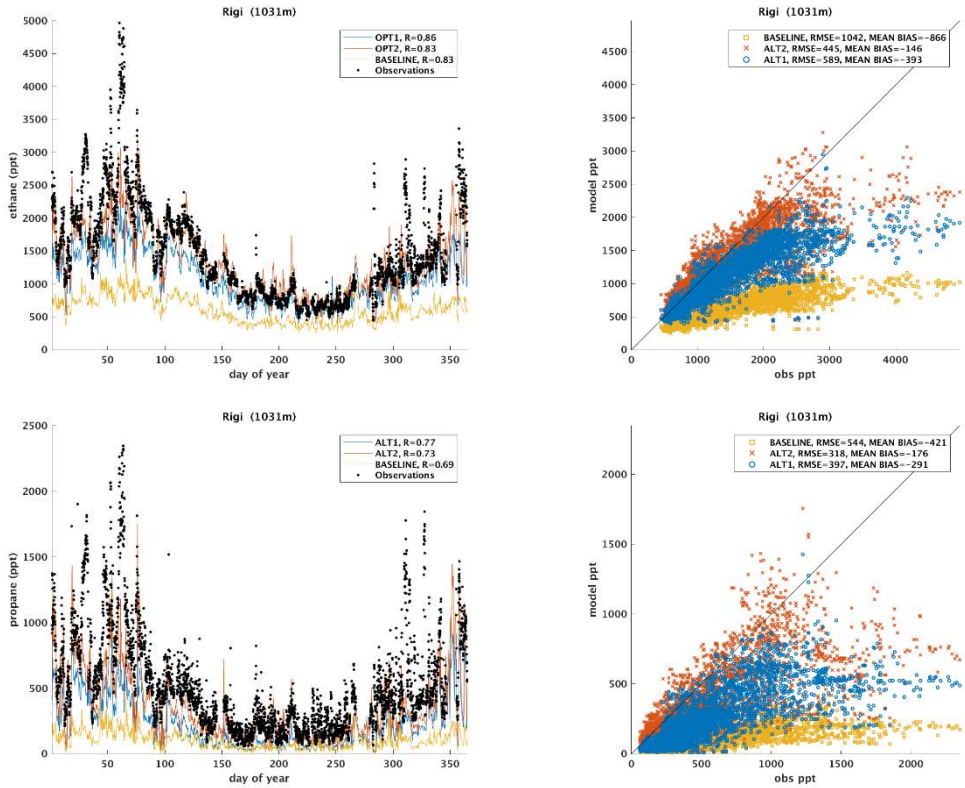

Figure S7: Comparison of modeled and observed ethane and propane for some non-Arctic European stations for the year 2011. All data were collected under the framework ACTRIS and EMEP, except Black Sea, Mace Head, and Baltic Sea, which were reported to GAW-WDCG by NOAA/INSTAAR. All data were accessed from the data bases in May 2017.

Table S2: Statistics for the ethane comparisons in Figures S5-S7.

	Mean R			Mean RMSE			Mean bias		
	Baseline	ALT1	ALT2	Baseline	ALT1	ALT2	Baseline	ALT1	ALT2
Arctic*	0.90	0.91	0.91	814	312	653	-687	56	479
U.S./Canada[δ]	0.78	0.86	0.83	785	358	413	-604	-57	87
Europe[†]	0.78	0.79	0.79	1083	595	920	-879	-93	567

*The statistics for the Tiksi station (only measurements for part of the year) are redrawn in the calculation of the regional mean. [δ]The statistics for the stations Lac La Biche (reasonable model performance except two extreme pollution episodes) and Southern Great Plains (general large model underestimation) are redrawn in the calculation of the regional mean. Due to the mentioned discrepancies these stations have poorer model performance, which means that they would totally dominate the calculated regional means for RMSE and bias. Possible reason for the poor model performance at Southern Great Plains is discussed in the main text. [†]For Europe the high altitude station Rigi is shown in Figure S6 as a representative for several alpine station in Europe (not shown). The statistics for Rigi is not included in the regional mean since this station is less representative of surface airmasses (regional emissions) than the other stations.

Table S3: Statistics for the propane comparisons in Figures S5-S7.

	Mean R			Mean RMSE			Mean bias		
	Baseline	ALT1	ALT2	Baseline	ALT1	ALT2	Baseline	ALT1	ALT2
Arctic*	0.84	0.89	0.90	453	307	459	-312	130	266
U.S./Canada[δ]	0.67	0.70	0.64	458	298	316	-329	-149	-36
Europe[†]	0.77	0.78	0.79	685	418	526	-569	-224	176

*The statistics for the Tiksi station (only measurements for part of the year) are redrawn in the calculation of the regional mean. [δ]The statistics for the stations Lac La Biche (reasonable model performance except two extreme pollution episodes) and Southern Great Plains (general large model underestimation) are redrawn in the calculation of the regional mean. Due to the mentioned discrepancies these stations have poorer model performance, which means that they would totally dominate the calculated regional means for RMSE and bias. Possible reason for the poor model performance at Southern Great Plains is discussed in the main text. [†]The statistics for the Black Sea station (reasonable model performance except one extreme pollution episode) are redrawn in the calculation of the regional mean. The high altitude station Rigi is shown in Figure S7 as a representative for a number of alpine station in Europe (not shown). The statistics for Rigi is neither included in the regional measn since this station is less representative of surface airmasses (regional emissions) than the other stations.

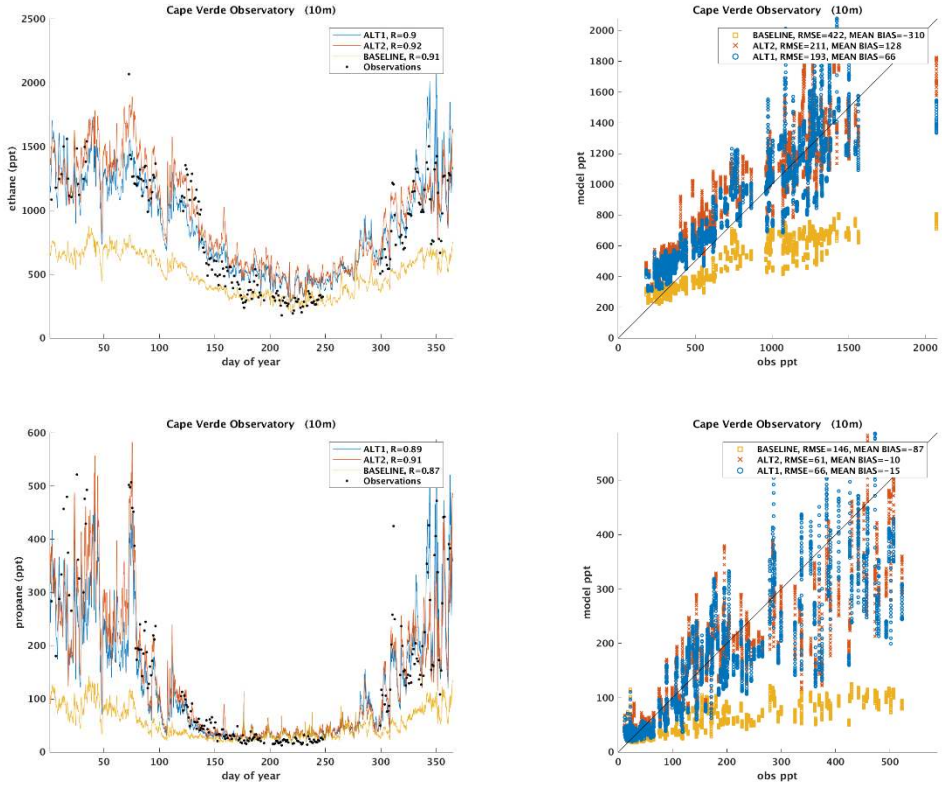

Figure S8: Comparison of modeled and observed ethane and propane at Cape Verde for the year 2011. The data were reported to GAW-WDCG by the University of York, and accessed in May 2017.

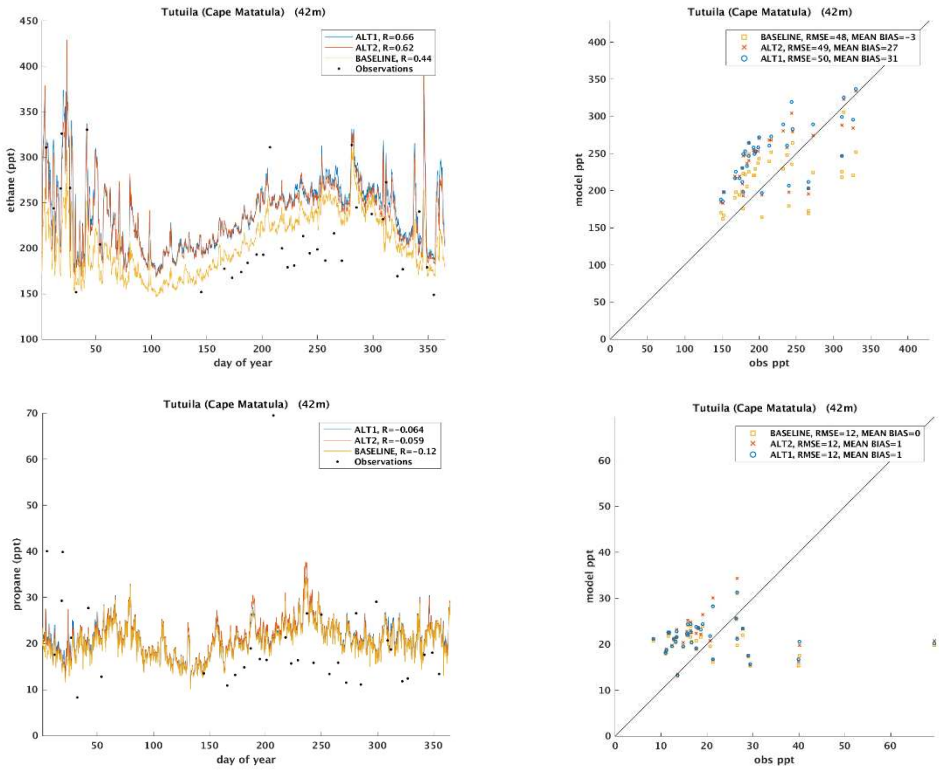

Figure S9: Comparison of modeled and observed ethane and propane at Samoa for the year 2011. The data were reported to GAW-WDCG by NOAA/INSTAAR, and accessed in May 2017.

OH sensitivity study

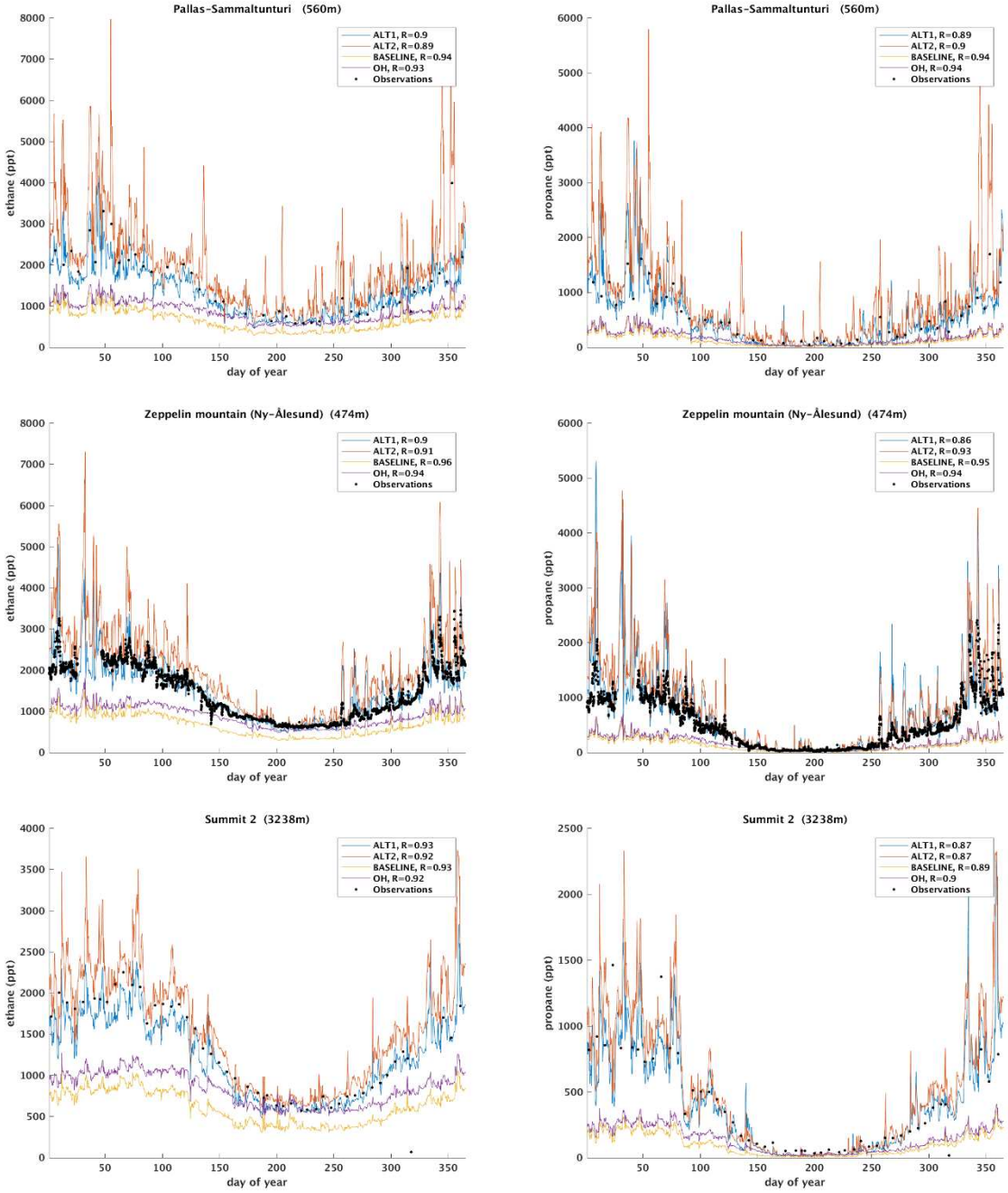

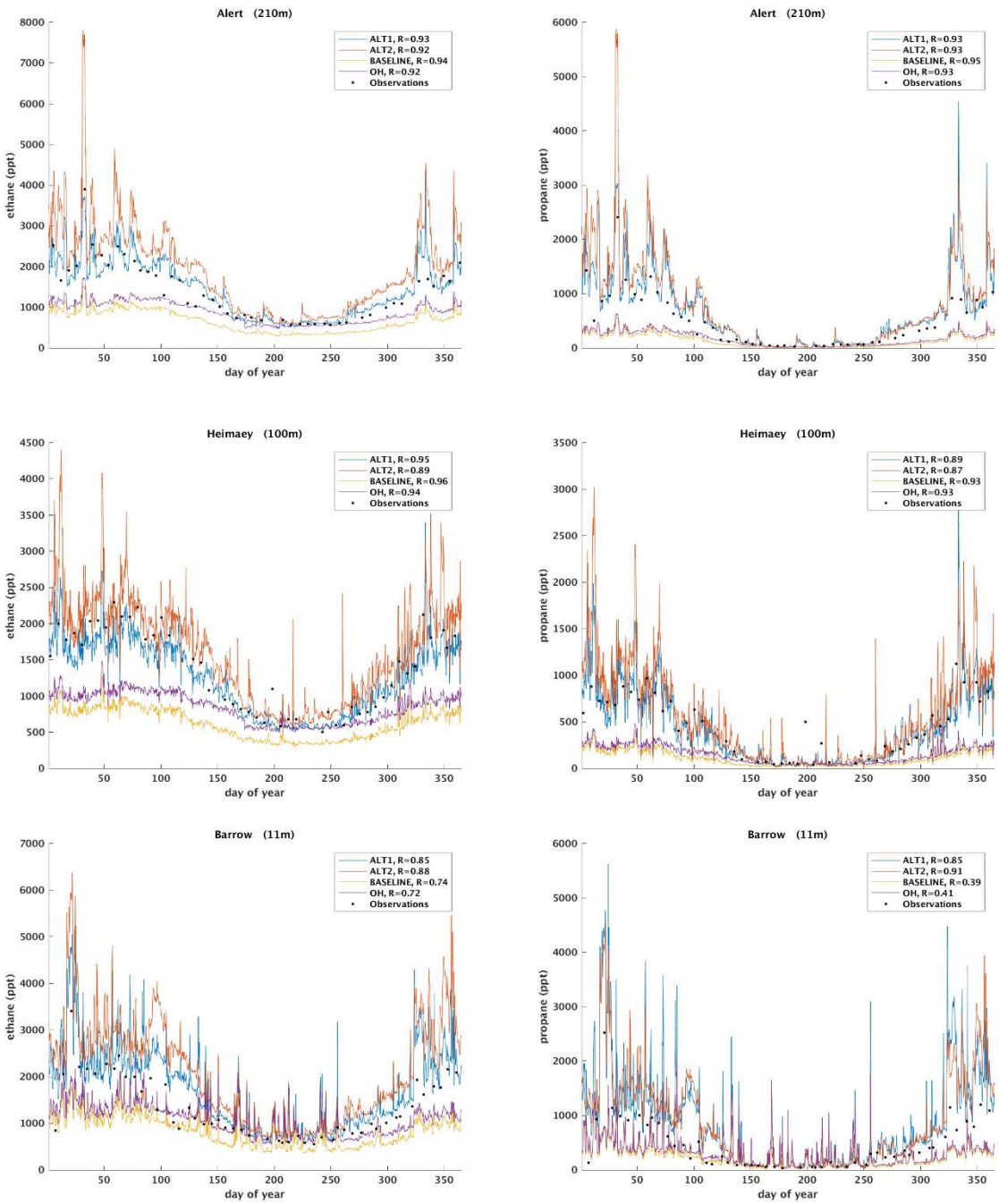
Alert (210m)
ALT1, R=0.93
ALT2, R=0.92
BASELINE, R=0.94
OH, R=0.92
Observations
ethane (ppt)
day of year
Alert (210m)
ALT1, R=0.93
ALT2, R=0.93
BASELINE, R=0.95
OH, R=0.93
Observations
propane (ppt)
day of year
Heimaey (100m)
ALT1, R=0.95
ALT2, R=0.89
BASELINE, R=0.96
OH, R=0.94
Observations
ethane (ppt)
day of year
Heimaey (100m)
ALT1, R=0.89
ALT2, R=0.87
BASELINE, R=0.93
OH, R=0.93
Observations
propane (ppt)
day of year
Barrow (11m)
ALT1, R=0.85
ALT2, R=0.88
BASELINE, R=0.74
OH, R=0.72
Observations
ethane (ppt)
day of year
Barrow (11m)
ALT1, R=0.85
ALT2, R=0.91
BASELINE, R=0.39
OH, R=0.41
Observations
propane (ppt)
day of year

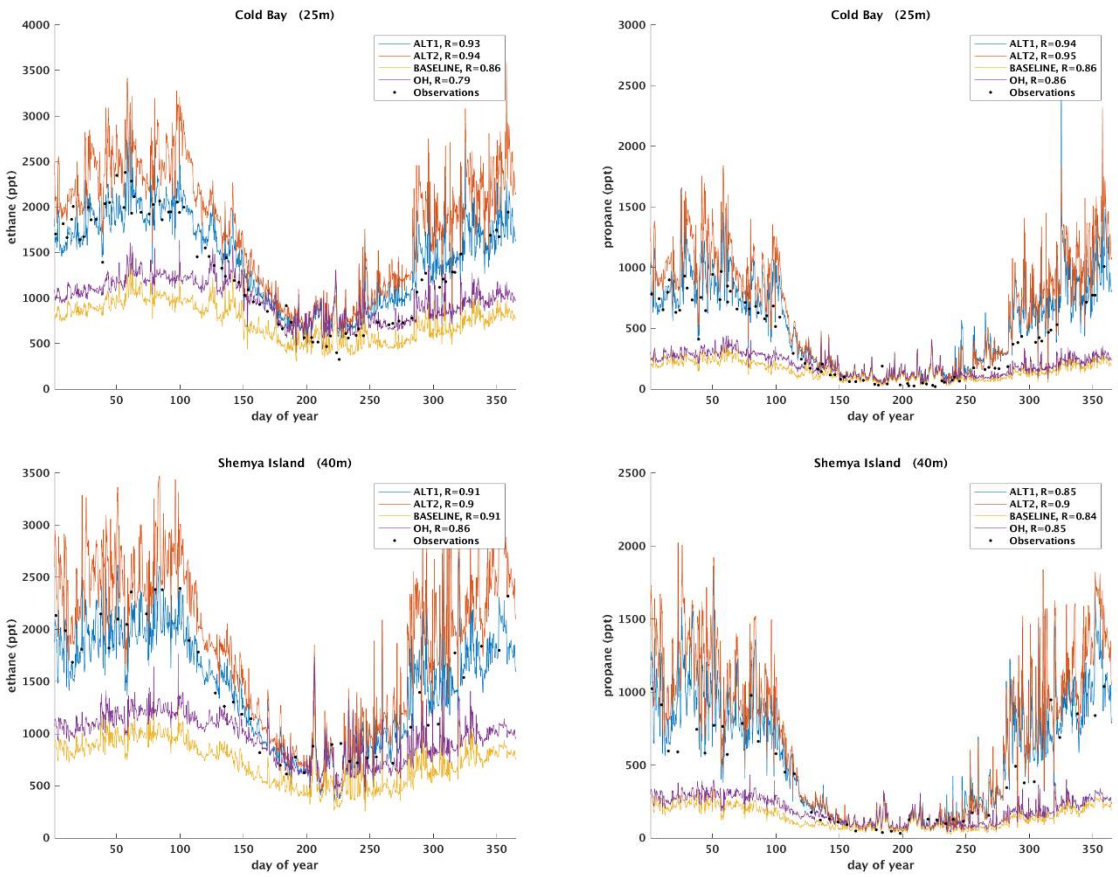

Figure S10: Comparison of modeled and observed ethane and propane for Arctic stations for the year 2011. The OH sensitivity simulation is plotted in purple. Zeppelin data were collected under the framework of ACTRIS, and the remaining sites were reported to GAW-WDCGG by NOAA/INSTAAR, and were accessed in May 2017.

Halogen chemistry and uncertainties

Reactions with halogens might be an atmospheric loss process for NMHCs of some importance, with chlorine radical reactions being the far most important[8]. For halogens, little experimental and observational data exist and there is a large knowledge gap regarding the complex interactions with aerosols. We have therefore not included oxidation of ethane and propane by halogens in the model. In one of the first model studies that have done so, ref. 8 estimates that chlorine accounts for 27 and 15 % of the global loss of ethane and propane, respectively. In ref. 8 the total increase in atmospheric chemical loss of ethane and propane is less than indicated by these numbers since the inclusion of halogens (chlorine, bromine, iodine) causes a compensating 8.2 % reduction in the global mean OH concentration.

Uncertainties in baseline and alternative anthropogenic emission inventories

Complete quantitative uncertainty estimates do not currently exist for the CEDS CMIP6 inventory[1] used in our baseline simulation. In CEDS CMIP6[1] the uncertainties in global total anthropogenic CO_2 and SO_2 emissions are estimated to be around 10 %, whereas they typically are 100 % for carbonaceous aerosols. The emission uncertainties for CO, NO_x, and NMHCs are stated to be in between these numbers. Based on that, we assume an emission uncertainty of ± 60 % for anthropogenic emissions of ethane and propane in the CEDS CMIP6 inventory used in our baseline simulations. This agrees quite well with the estimates for the older EDGARv3 (http://themasites.pbl.nl/tridion/en/themasites/edgar/documentation/uncertainties/index-2.html), where the uncertainties for individual sectors fall in the categories medium (around 50 %) and high (around 100 %). Based on the span in the approximate uncertainty numbers reported in CEDS CMIP6[1] and EDGAR (above link to documentation) we further assume that our selected CEDS CMIP6 uncertainty estimate (± 60 %) has a confidence level of one standard deviation (68 %).

There are very few quantitative datasets available on uncertainties in other global standard community emission inventories. It is therefore difficult to estimate the combined uncertainty for the eight other inventories shown in Figures 1b, S1 and S11. We expect the emission uncertainties in each of these older inventories to be equal or larger than that of the CEDS CMIP6 state of the art inventory.

For the new fugitive fossil fuel emission dataset in the ALT1 inventory the uncertainty in emissions from associated gas flow and handling is based on the uncertainty estimates in Table 3 of ref. 9. For the uncertainty in emissions from unintended leakage, IPCC default factors[10] were modified to -50% of the IPCC low-end and to +10% of the IPCC high-end. The ranges for the IPCC default factors are very large, in particular the high-end value for developing countries, which is likely to reflect emissions from occasional "super-emitters", that are hardly representative for the global scale. The uncertainty range for leakage during shale gas extraction was set to be from 2% to 5%. For coal emissions the low and high estimates of ref. 11 is used. The overall uncertainty range for the ALT1 fugitive fossil fuel emissions is -28 % to +38 % for both ethane and propane with a confidence level of one standard deviation (68 %).

The ALT2 inventory emission uncertainties for the fugitive fossil fuel emissions are from ref. 11. Based on top down studies[12] the low gas scenario from ref. 11 is considered most likely. Our upper total fugitive emission estimate uses the combination emissions low gas and high coal and oil, while our lower total fugitive emission estimate has the combination low gas, coal, and oil. The overall uncertainty in the fugitive fuel emissions in ALT2 range from -27 % to +30 % for both ethane and propane with a confidence level of one standard deviation (68 %).

In the fugitive fossil fuel datasets in the ALT1 and ALT2 inventories the relative uncertainties (around ± 30 %) are about halved compared to that assumed (± 60 %) above for the CEDS CMIP6 inventory. The reason is that the ALT1 and ALT2 datasets are based on novel approaches to quantify and attribute methane and NMHC emissions and take much better into account that the emission factors from venting and flaring of associated gas released during extraction vary considerably across different oil, coal and gas fields in the world. The main text and methods section provide further information on differences in data quality, calculation methods, etc.

In the ALT1 and ALT2 simulations we use conservative low estimates of fugitive fossil fuel emissions. Due to potential double-counting[11] we assume full overlap with geologic seepage emissions: Conservative low estimates = Best estimates with geologic seepage emissions subtracted (see Methods for details). The anthropogenic (excluding biomass burning) ethane emissions used in the baseline, ALT1, and ALT2 model simulations are shown in Figure S11 together with uncertainty ranges calculated based on the estimates discussed in this section.

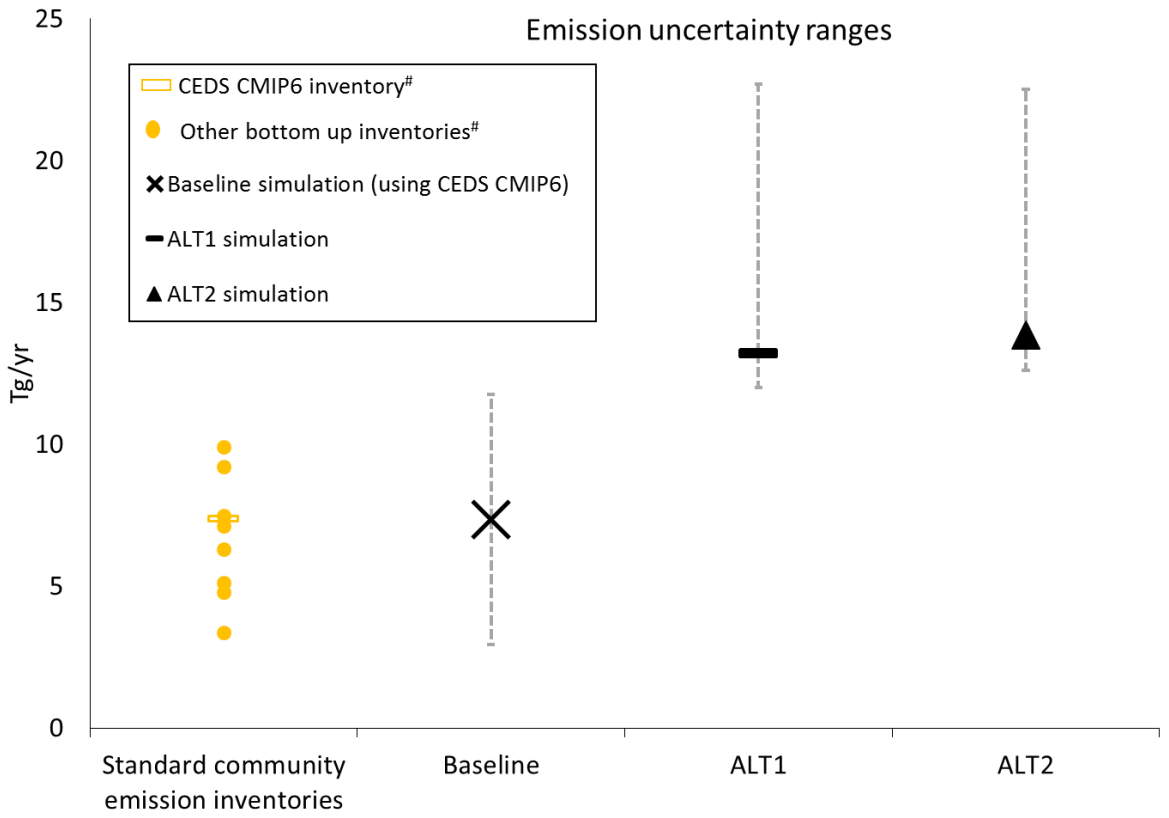

Figure S11: Error bars: Ethane emission uncertainties for anthropogenic (excluding biomass burning) inventories (Baseline, ALT1, ALT2) used in this study. The confidence level is one standard deviation. Explanation for deriving these estimates is provided above. #Global total anthropogenic emissions (excluding biomass burning) in 9 standard community emission inventories. CEDS CMIP6 (used in baseline this study), HTAPv2, RETRO, POET, Edgar 3.2 FT, CMIP5 (Average of MACCITY, ACCMIP, RCP2.6, RCP4.5, RCP6, and RCP8.5) (as reported and referenced in the ECCAD database: http://eccad.aeris-data.fr/), ARCTAS (as reported by ref. 2), EDGAR4.3.2 (as reported by ref. 3) , and new inventory in ref. 4.

Impacts on air pollutants

Modeled baseline ozone values are compared to surface ozone measurements in Figure S12. This section provides an overview of the regional features (main text focus on general features). In Europe the modeled ozone levels are very close to the measured ones. The poorest model performance is in Korea, the eastern U. S., and west of central Africa. For Korea and the eastern U. S., a likely cause is that current global model resolutions are not fully capable of reproducing the high spatial heterogeneity in NO_x ($NO+NO_2$). For central Africa, the regional influence of biomass burning appears too high.

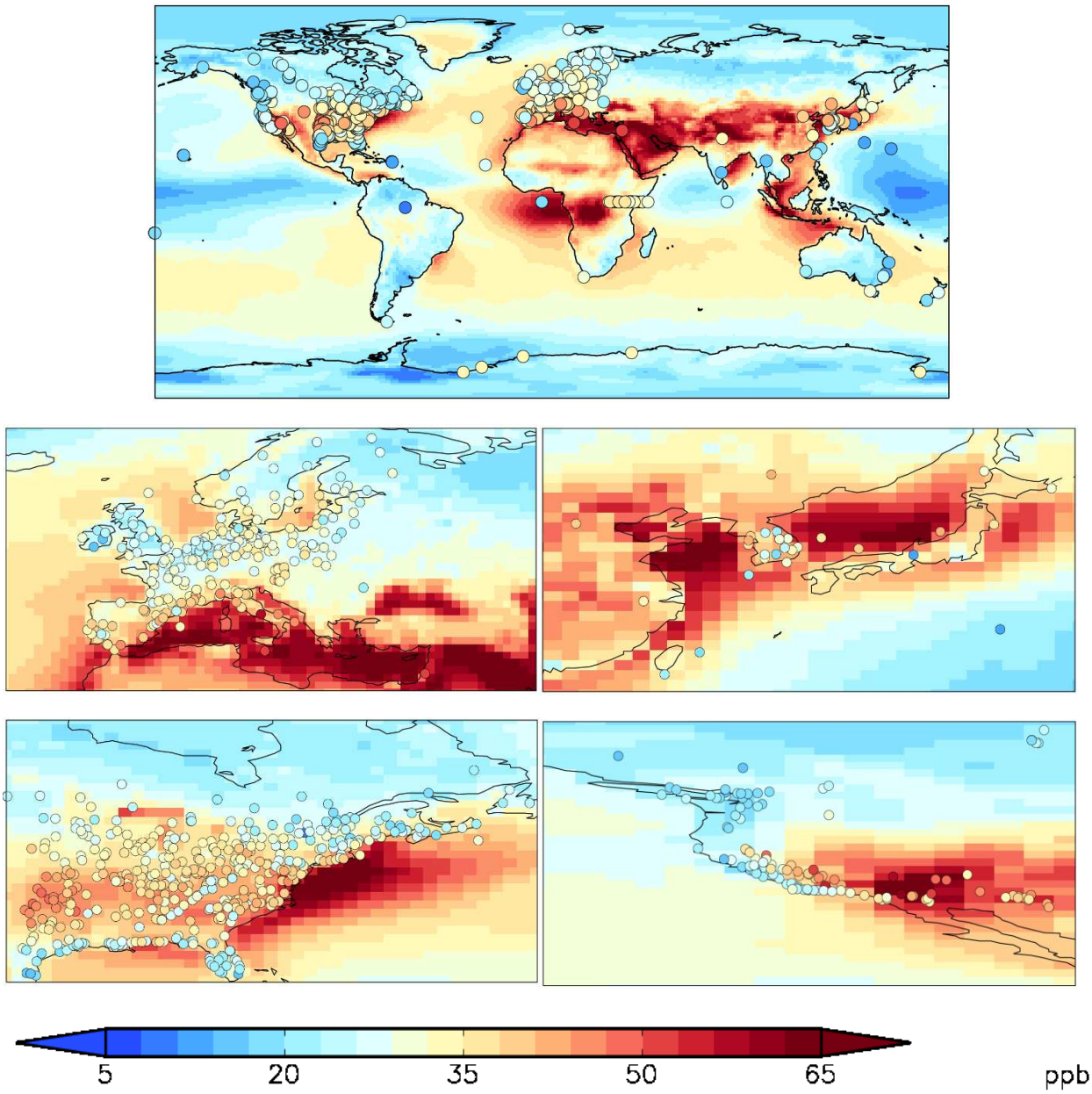

Figure S12: Comparison of modeled (baseline simulation, shown with background colors) and observed surface (color-filled circles) ozone (ppb) averaged over the period June-August 2011. Model data for the lowest model layer were used. Upper panel: Global comparison. Mid panels: Zooming in on Europe and eastern Asia. Lower panel: Zooming in on eastern and western northern America. Observed seasonal ozone averages are from the TOAR database[13] and filtered to exclude urban and suburban stations, and stations situated above 500 m.a.s.l.

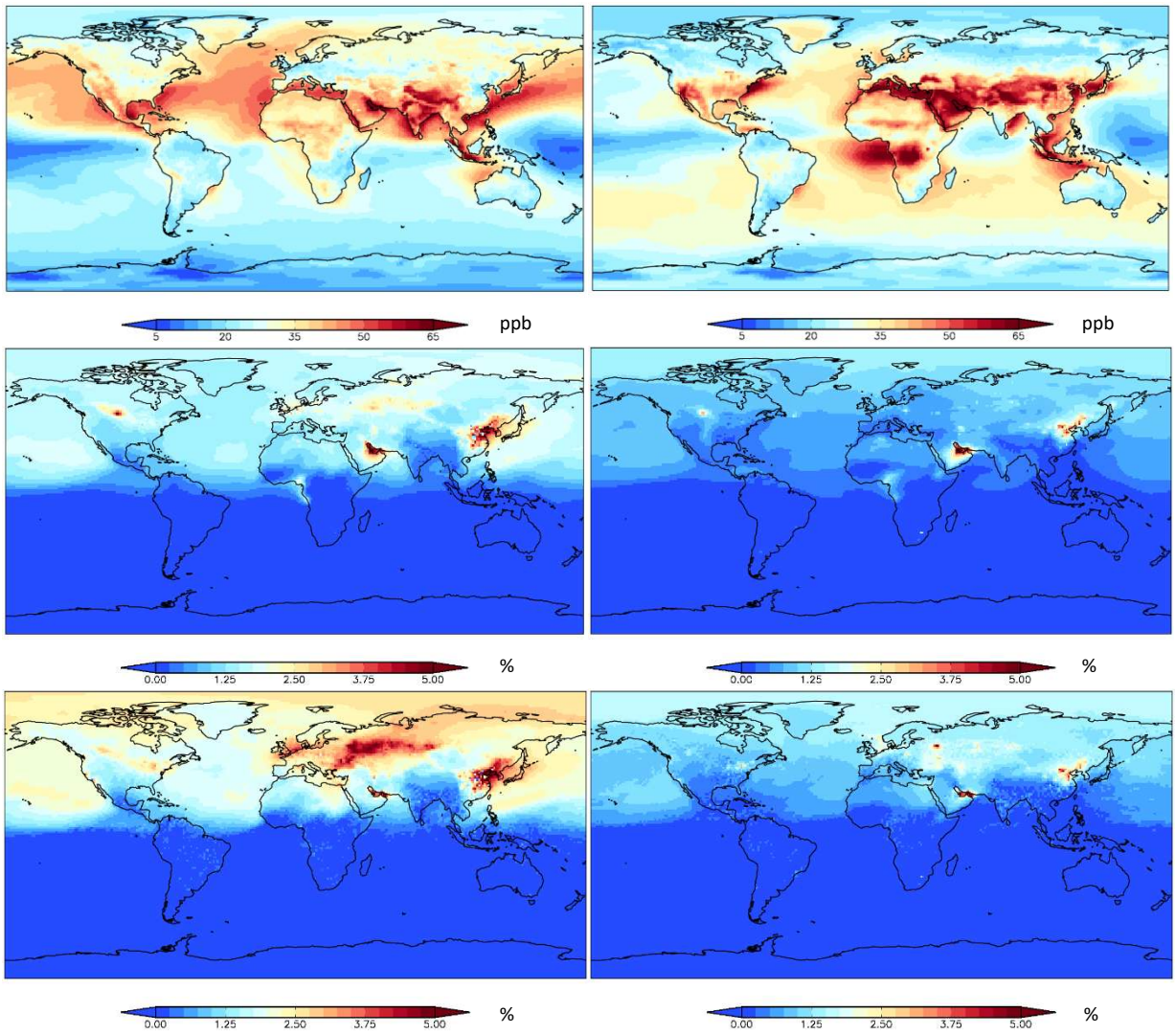

Figure S13: Upper panel: Ozone (ppb) in the lowest model layer in the baseline simulation. Left: March-May mean. Right: Jun-Aug mean. Mid panel: Ozone difference (%) relative to Baseline in ALT1 simulation. Left: March-May mean. Right: Jun-Aug mean. Lower panel: Ozone difference (%) relative to Baseline in ALT2 simulation. Left: March-May mean. Right: Jun-Aug mean.

In addition to effects on surface ozone (main text and Figures S12-13), the higher emissions in ALT1 and ALT2 impacts the major air pollutants NO_2, PAN and CO. Surface NO_2 differences between ALT1, ALT2 and baseline are up to ± 10 % (± 6 ppb) in Dec-Feb in the Northern Hemisphere (Figure S14). The NO_2 perturbations are mainly caused by higher PAN (10-20 % in the Northern Hemisphere, Figure S14) in ALT1 and ALT2. Atmospheric ethane and propane oxidation and subsequent reactions with NO_2 are large sources for PAN formation, and PAN is an important NO_2 reservoir[14]. PAN islin generated in emission source areas, transported to warm regions, and thermally decomposing resulting in higher NO_2 in such regions in ALT1 and ALT2 compared to the baseline (Figure S14). When temperatures are low as at high latitudes in wintertime (Figure S14) more NO_2 is inactivated in the form of PAN. The changes in CO (not shown) are small and in the range 0-5 %.

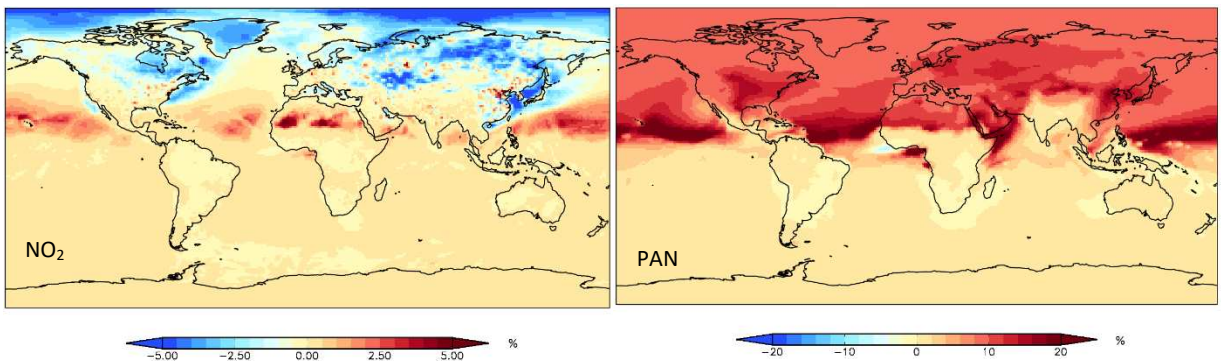

Figure S14: Left: Mean Dec-Feb change in surface (lowest model layer) NO_2 (%) relative to baseline for ALT1 simulation. Right: Same for PAN.

References

1 Hoesly, R. M. *et al.* Historical (1750–2014) anthropogenic emissions of reactive gases and aerosols from the Community Emission Data System (CEDS). *Geosci. Model Dev. Discuss.* **2017**, 1-41 (2017).

2 Emmons, L. K. *et al.* The POLARCAT Model Intercomparison Project (POLMIP): overview and evaluation with observations. *Atmos. Chem. Phys.* **15**, 6721-6744 (2015).

3 Huang, G. *et al.* Speciation of anthropogenic emissions of non-methane volatile organic compounds: a global gridded data set for 1970–2012. *Atmos. Chem. Phys.* **17**, 7683-7701 (2017).

4 Tzompa-Sosa, Z. A. *et al.* Revisiting global fossil fuel and biofuel emissions of ethane. *Journal of Geophysical Research: Atmospheres* **122**, 2493-2512 (2017).

5 Helmig, D. *et al.* Reversal of global atmospheric ethane and propane trends largely due to US oil and natural gas production. *Nature Geosci* **9**, 490-495 (2016).

6 Franco, B. *et al.* Evaluating ethane and methane emissions associated with the development of oil and natural gas extraction in North America. *Environmental Research Letters* **11**, 044010 (2016).

7 Etiope, G. & Ciccioli, P. Earth's Degassing: A Missing Ethane and Propane Source. *Science* **323**, 478-478 (2009).

8 Sherwen, T. *et al.* Global impacts of tropospheric halogens (Cl, Br, I) on oxidants and composition in GEOS-Chem, Atmos. Chem. Phys. **16**, 12239-12271 (2016).

9 Höglund-Isaksson, L. Bottom-up simulations of methane and ethane emissions from global oil and gas sysreftems 1980 to 2012. *Environmental Research Letters* **12**, 024007 (2017).

10 IPCC. Vol. 2 *IPCC Guidelines for National Greenhouse Gas Inventories* Tables 4.2.4 and 4.2.5 (IPCC, Japan, 2006).

11 Schwietzke, S., Griffin, W. M., Matthews, H. S. & Bruhwiler, L. M. P. Global Bottom-Up Fossil Fuel Fugitive Methane and Ethane Emissions Inventory for Atmospheric Modeling. *ACS Sustainable Chemistry & Engineering* **2**, 1992-2001 (2014).

12 Schwietzke, S., Griffin, W. M., Matthews, H. S. & Bruhwiler, L. M. P. Natural Gas Fugitive Emissions Rates Constrained by Global Atmospheric Methane and Ethane. *Environ. Sci. Technol.* **48**, 7714-7722 (2014).

13 Schultz, M. G. *et al.* in *Supplement to: Schultz, MG et al. (in press): Tropospheric Ozone Assessment Report: Database and Metrics Data of Global Surface Ozone Observations. Elementa, https://doi.org/10.1525/elementa.244* Custom 8 (PANGAEA, 2017).

14 Fischer, E. V. *et al.* Atmospheric peroxyacetyl nitrate (PAN): a global budget and source attribution. *Atmos. Chem. Phys.* **14**, 2679-2698 (2014).